

In presenting this thesis in partial fulfillment of the requirements for an advanced degree at Idaho State University, I agree that the Library shall make it freely available for inspection. I further state that permission to download and/or print my thesis for scholarly purposes may be granted by the Dean of the Graduate School, Dean of my academic division, or by the University Librarian. It is understood that any copying or publication of this thesis for financial gain shall not be allowed without my written permission.

Signature _____

Date_____

**TEMPERATURE EFFECTS ON THE
ISU-AGN-201 REACTOR**

by

Ryan Loveland

A thesis

submitted in partial fulfillment

of the requirements for the degree of

Master of Science in Nuclear Science and Engineering

Idaho State University

December 2015

To the Graduate Faculty:

The members of the committee appointed to examine the thesis of Ryan K.
Loveland find it satisfactory and recommend that it be accepted.

Dr. Jay F. Kunze,
Major Advisor

Dr. George Imel,
Committee Member

Dr. Brian Williams,
Graduate Faculty Representative

ACKNOWLEDGEMENTS

It is hard to thank all of the people that have assisted and encouraged me during my time at Idaho State University.

I believe my advisor Dr. Kunze to be one of the greatest people I have ever had the pleasure of knowing. His love for his students and the nuclear engineering program at ISU is apparent. I know that in addition to me, many at ISU, in the Pocatello community and his church have been greatly blessed by the countless hours of service he so readily performs. As a mentor there are none better. I will miss his brilliant mind and vast experience.

Dr. Williams' undergraduate thermodynamics class is still a favorite of mine. His enthusiasm and clarity of instruction ignited an interest in the topic that has only increased over time. Indeed, all of the classes I have taken from him have been particularly enjoyable. I have also been the recipient of his charity and good nature. I feel privileged to have him as a member of my committee.

I would like to thank Dr. Imel for stepping in at the last minute to complete my committee. He and the entire engineering faculty have always been available and willing to help me in a professional and intelligent manner. For this I am very grateful.

The engineering office staff deserves more recognition than I can give them. They have always been willing to quickly aid in any problem I have had for them. The reactor staff and operators have been equally as helpful. I cannot name all of the friends I have made down there over the years.

I would like to thank my parents for their support and continual encouragement.

Finally I must thank God and my wife, Kaylene. Both have had exercised extreme patience with me and lifted me up through this process. I particularly appreciate Kaylene taking care of our 3 children and all the household responsibilities when I have needed to work on this thesis. I love her dearly.

CONTENTS

LIST OF FIGURES.....	viii
LIST OF TABLES.....	ix
ABSTRACT.....	x
VITA.....	xi
1 INTRODUCTION.....	1
2 LITERATURE REVIEW	3
3 REACTOR PROPERTIES	4
4 ANALYTIC SOLUTION.....	10
4.1 Formation.....	10
4.2 Analysis of the Analytic Solution.....	19
5 NUMERICAL SOLUTION	24
5.1 Formation.....	24
5.2 Analysis of Numerical Solution	26
6 CHANGE IN REACTIVITY WITH TEMPERATURE	28
6.1 Change in Thermal Utilization Factor.....	28
6.2 Thermal Expansion.....	30
6.3 Doppler Effect	30
6.4 Thermal Non-Leakage Probability.....	31
6.5 DISNEL Validation.....	33
6.6 Theoretical Reactivity Changes from Numeric Profiles	34
7 EXPERIMENT	38
7.1 Initial Experiment.....	38
7.2 Temperature and Reactivity Measuring Experiment.....	38
7.3 Experimental Results	41
8 COMBINED RESULTS AND ANALYSIS.....	45
9 CONCLUSION.....	49
REFERENCES.....	50
APPENDIX A – MARK GAINES REPORT	52
APPENDIX B – POWER CALIBRATION	55

APPENDIX C – GOLD FOIL EXPERIMENT	56
APPENDIX D – MATLAB CODES	59
APPENDIX E – DISNEL CODES	69

LIST OF FIGURES

Figure 3-1 Fuel Disk Showing Fuel Rod Holes (2)	4
Figure 3-2 Cross Section of Reactor Tank from Above	6
Figure 3-3 Cross Section of Core Tank Showing Additional Supporting Structures	8
Figure 4-1 Temperature Change in Materials Outside the Core Operating at 5 W	13
Figure 4-2 Plot of Analytic Solution.....	20
Figure 4-3 Normalized Flux Profile.....	21
Figure 4-4 Flux Profile with Values for Bessel Function Added	22
Figure 4-5 Measure and Assumed Flux Profiles, with Equal Volume Under the Curves	23
Figure 5-1 Steady State Radial Temperature Profile from Cylindrical Analysis, at $z = 0$	26
Figure 5-2 Steady State Temperature Profile from Spherical Analysis.....	27
Figure 6-1 Values of g as a Function of Temperature (13).....	29
Figure 6-2 Doppler Broadening of Resonance with Increased Temperature (15).....	31
Figure 6-3 Cross Section of Hydrogen in Paraffin (16).....	32
Figure 6-4 100W Steady State Temperature Profile.....	37
Figure 7-1 Core Temperature Measuring Device	39
Figure 7-2 Thermocouples on the Polyethylene Tube	39
Figure 7-3 Thermocouple Reader	40
Figure 7-4 Recorded Change in Temperatures for all Thermocouples.....	42
Figure 7-5 Recorded Change in Temperatures for Thermocouples Excluding 2.54 cm ..	43
Figure 7-6 Measured Reactivity Insertion vs Time	44
Figure 8-1 Temperature Profiles at 417 Minutes	45
Figure 8-2 Change in Temperature at 5.08 cm Radially.....	46
Figure 8-3 Measured and Theoretical Reactivity Insertion vs Time	47
Figure 8-4 Measured and Empirical Reactivity Insertions	48

LIST OF TABLES

Table 3-1 Properties of UO ₂ , Polyethylene and the Homogenous Core.....	5
Table 3-2 Atom Densities of Core Materials	5
Table 3-3 Properties of materials surrounding the reactor core.....	7
Table 6-1 Reactivity Contribution of Individual Temperature Effects.....	34
Table 6-2 Comparison of k with Number of Temperature Regions	35
Table 6-3 Calculated Average Core Temperatures for Each Time Step	36

ABSTRACT

This thesis examines temperature change in the Idaho State University AGN-201 reactor and its subsequent affect on reactivity. A theoretic temperature profile is derived mathematically by assuming a bare cylindrical core power distribution. The temperature profile is improved upon numerically using finite difference and a measured power distribution. The temperature profile is then used in conjunction with the reactor physics code “DISNEL” to determine the theoretic change in reactivity with time. DISNEL is also used to explore what reactor characteristics most influence the reactor temperature coefficient of reactivity and compare the isothermal coefficient to the dynamic coefficient. An experiment is designed and conducted to measure the temperature and reactivity changes in the core during operation. The experimental data is then compared to the theoretical predictions.

VITA

Ryan Loveland is a native of Pocatello, Idaho. In 2008 he received his bachelor's degree from Idaho State University in Mechanical and Nuclear Engineering. He has been a licensed Senior Reactor Operator for the ISU AGN-201 reactor for 7 years. His research interests include reactor physics, thermal-hydraulics, and numerical methods. He is active in the community as a member of the Pocatello Planning and Zoning Commission.

1 INTRODUCTION

Idaho State University has operated an Areojet General Nucleonics model number 201M nuclear reactor since 1965. (1) The (AGN-201) is a small training reactor that functions as a laboratory tool to train nuclear engineering students. It is a safe reactor that operates at low powers and is an excellent resource for training students in all aspects of nuclear operation, physics and design.

Recent graduate research that has been done on the reactor includes the development of a benchmark model of the reactor for inclusion in the *International Handbook of Evaluated Reactor Physics Benchmark Experiments* (2), and a project to more accurately determine the effective delayed neutron fraction and the neutron generation time (3).

One aspect of the AGN-201 reactor which has not been adequately described in the benchmark data is the temperature coefficient of reactivity. Particularly, there has never been a precise quantification of the reactivity feedback due to temperature experienced during reactor operation. This was a particular problem during some of the long reactor runs of the Nuclear Energy University Partnership oscillator project (4) of which the previously mentioned reactor parameters project was only a small part.

To understand the dynamic temperature coefficient, a transient temperature profile of the core was desired. The core of the AGN-201 is unique in that geometrically it is closer to a homogenous right cylinder than any other functioning reactor. This makes the reactor ideal for testing simple mathematical models.

Using the cylindrical conduction Equation and the theoretical power distribution of a bare reactor (5), a mathematical solution of the temperature profile was created. The mathematical model was further refined numerically using finite difference methods and the power distribution data measured from the reactor.

An experiment was designed to measure the temperature distribution as well as the change in reactivity of the core while the reactor was operated at high power for long periods of time.

The reactor physics code DISNEL and analytical method was used to analyze the effects of the theoretical temperature profile on the reactivity change in the core. Additionally, DISNEL was used to examine contrast between the isothermal temperature coefficient and the dynamic temperature coefficient, as well as to analyze the contribution of various reactor physics characteristics to the temperature coefficient.

2 LITERATURE REVIEW

The temperature coefficient of reactivity recorded in the official licensing documents of the ISU AGN reactor is $-0.025\ \% \Delta k/kC$. (6)

A hazard summary report for AGN-201 was developed by Argonne National Laboratory in 1962. (7) It determined the steady state temperature while operating at a power of 100 mW would be $0.044\ ^\circ C$ by using the steady state spherical conduction equation. It assumed the driving function was the temperature distribution multiplied by the power density and divided by the average temperature. Additionally, it was assumed that the material surrounding the core is an infinite heat sink.

The hazard summary report also derived a temperature coefficient of reactivity of $-0.036\ \% \Delta k/kC$ by calculating partial coefficients with the assumption that the core acts as a bare reactor.

In 2010, Mark Gaines, an undergraduate student at Idaho State University, used a year's worth of the AGN-201 operator logs to plot the measured excess reactivity and the temperature for each reactor run. In his memorandum to the reactor staff, he concluded that a more accurate temperature coefficient would be $-0.03\ \% \Delta k/kC$. (8) The entirety of this report can be found in appendix A.

3 REACTOR PROPERTIES

The reactor core consists of nine circular polyethylene discs embedded with UO_2 power. Four of these fuel disks have four holes cut into them to facilitate the insertion of fueled control rods. Figure 3-1 shows how these holes are arranged in one of the fuel discs. The cutout for the bottom of the “glory hole” experimental port can also be seen in the picture.



Figure 3-1 Fuel Disk Showing Fuel Rod Holes (2)

An additional disk referred to as the Reactivity-Adding Disk (RAD), is a polyethylene disk with a quarter piece of the previously mentioned fuel disk material embedded in the middle. Gorham discussed the different reports of the dimensions of the fuel disks. She concluded that when installed the fuel discs and RAD form a right circular cylinder of 25.6 centimeters in diameter and 24.7 centimeters in height. (2) When the fuel rods are inserted to fill the voids left by the holes in the fuel disks [see Figure 3-1] the core is very close to a complete homogenous cylinder with the above mentioned dimensions and a volume of 12714 cm^3 .

The enrichment of the uranium in the reactor fuel is just under 20 percent U-235.

(6) The weight percent of U-235 in the UO_2 was calculated as 0.1745. The room temperature density of UO_2 is 10.97 g/cm^3 . (9) Using the weight percent of U-235, the mass of U-235 per cubic centimeter of UO_2 was calculated to be 1.914 g/cm^3 . This was applied to the 665g (2) critical mass of U-235 to determine the volume of UO_2 in the core. Table 3-1 lists properties of UO_2 , polyethylene and the homogenous core.

Table 3-1 Properties of UO_2 , Polyethylene and the Homogenous Core

	Volume cm^3	Mass G	Density g/cm^3	Specific Heat J/gK	Thermal Conductivity W/cmK
UO_2	347.45	3811.5	10.97 (9)	0.23381 (9)	0.08925 (9)
Polyethylene	12367	11872	0.96	2.25 (10)	0.0049 (10)
Mixed Core	12714	15684	1.234	1.760	0.0072

The specific heat of the core was calculated using a mass weighted average of the other two materials. The thermal conductivity is a volume weighted average.

The atom densities of the various elements in the core were calculated and are listed in Table 3-2.

Table 3-2 Atom Densities of Core Materials

Element	Atom Fraction atoms/(barn*cm)
U-235	1.3403×10^{-4}
U-238	5.3600×10^{-4}
Oxygen	1.3378×10^{-3}
Hydrogen	4.0189×10^{-2}

Carbon	8.0378×10^{-2}
--------	-------------------------

Figure 3-2 is the cross section of the reactor tank from above.

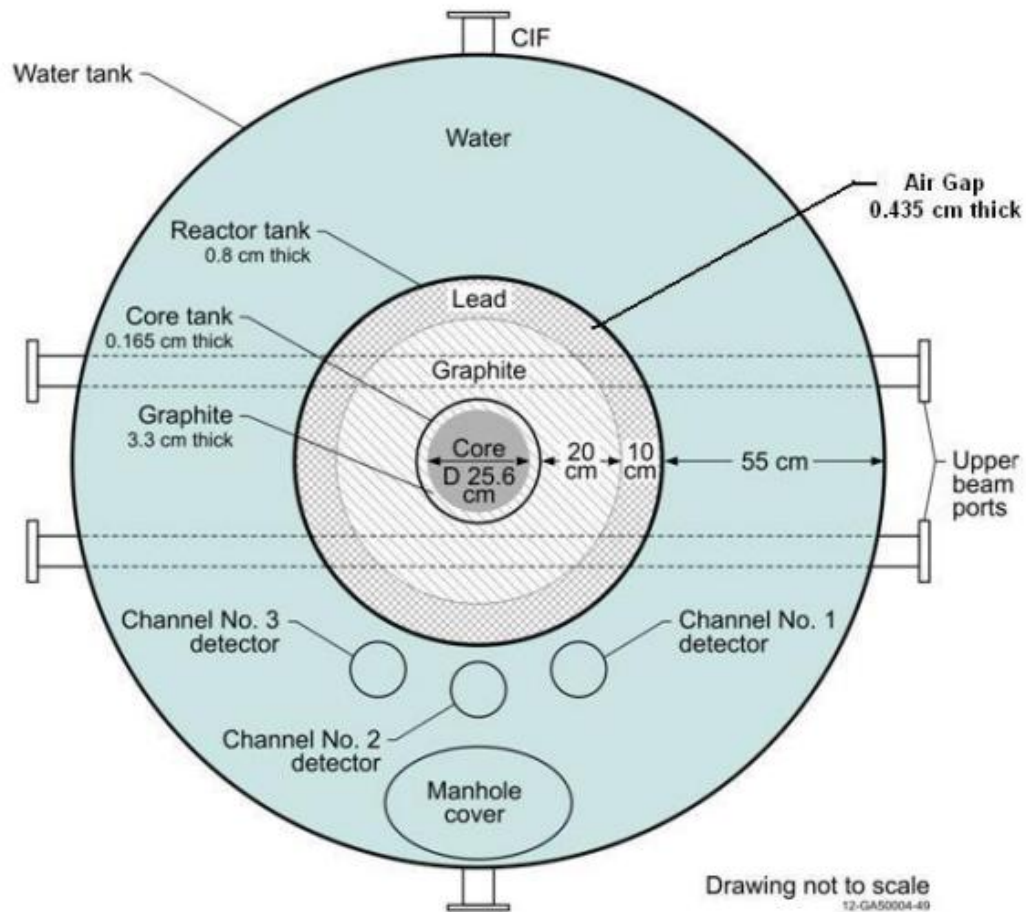


Figure 3-2 Cross Section of Reactor Tank from Above

Starting at the center and moving out there is the core and then a layer of graphite. The graphite and core are in a sealed core tank of aluminum. Beyond the core tank is another layer of graphite and a layer of lead all encapsulated in a stainless-steel tank. This tank is concentric within another larger tank that holds approximately 1000 gallons of water.

Table 3-3 lists the inner and outer radii as well as the thermal conductivity for each material. Because it is comparatively thin and aluminum has a high thermal conductivity, the core tank was neglected.

Table 3-3 Properties of materials surrounding the reactor core

Material	Inner Radius (cm)	Outer Radius (cm)	k (w/mK)
Polyethylene	0	12.8	0.3349
Graphite	12.8	37.5	80
Lead	37.5	47.5	35
Steel	47.5	48.3	16
Water	48.3	99	0.58

The reactor has five experimental ports into which material samples, detectors and other equipment can be inserted for experimentation purposes. The glory hole, as it is called, is a small 2.2 cm diameter aluminum pipe that runs through the longitudinal middle of the reactor core. Figure 3-1 shows that there is a spot cut out of that fuel disc to facilitate the glory hole. Additionally there are four beam ports that run tangent to the side of the reactor core and perpendicular to the glory hole. These ports pass through the reflector and do not penetrate the core itself.

The bottom of Figure 3-3 shows the control rods and the drive mechanisms that insert the control rods into the core.

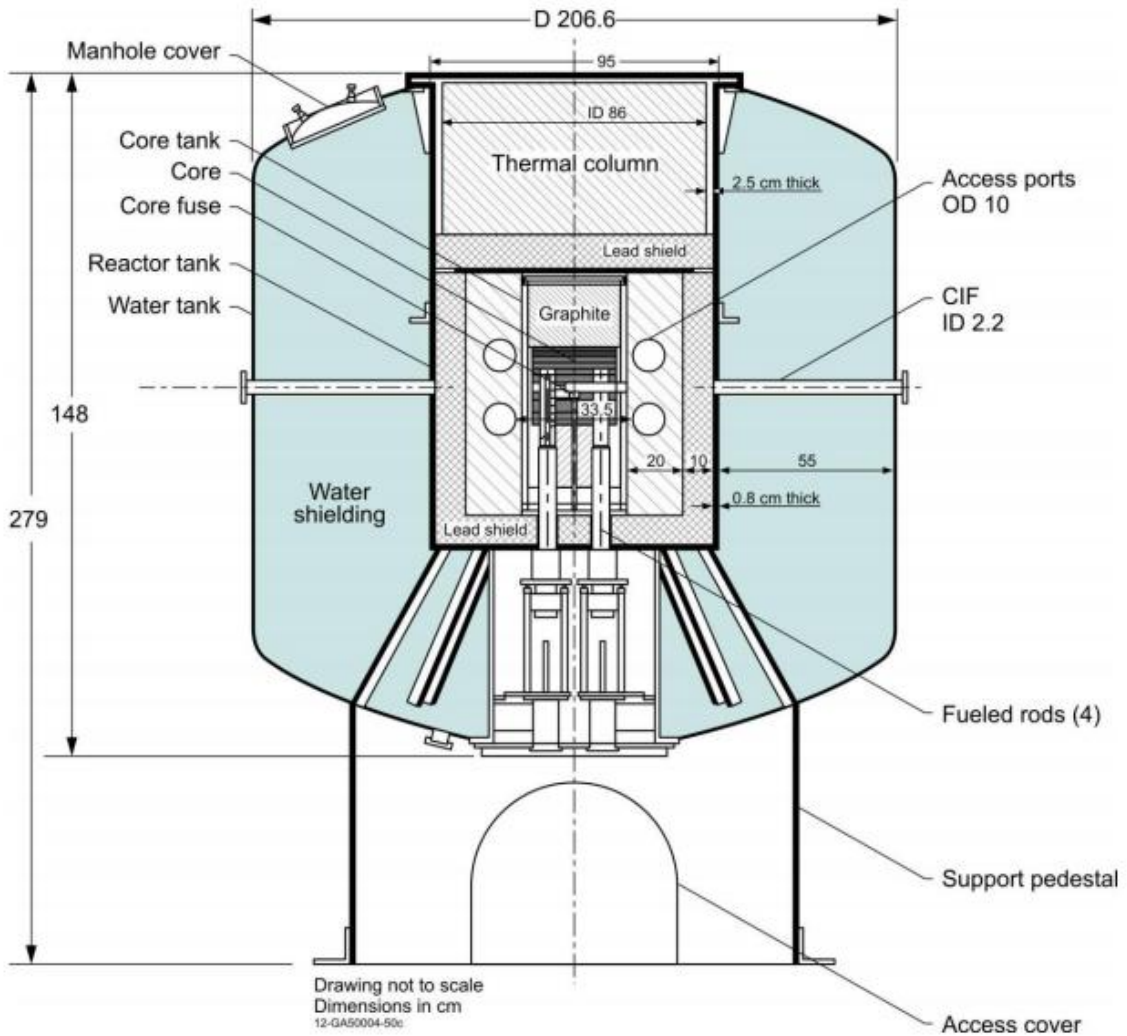


Figure 3-3 Cross Section of Core Tank Showing Additional Supporting Structures

There are four rods, three 4.7 cm in diameter and a smaller 2.3 cm fine rod. Two of the larger rods function as safety rods and are meant to be either fully inserted or fully withdrawn from the reactor core. The other two rods are used to control the neutron chain reaction. The reactor console indicates the position of these rods within the reactor core. The larger rod is used for coarse adjustments and the smaller for fine.

Three neutron detectors located in the water tank are shown in Figure 3-2. The signals they generate are indicated as channels 1 through 3 on the reactor console.

Channel 3 is used to determine the reactor power. Appendix B is the power calibration used at the time this report was conducted.

4 ANALYTIC SOLUTION

4.1 Formation

Since, the core of the AGN-201 is designed to closely resemble a homogenous cylinder, it is reasonable to attempt to find an analytical solution to the conduction heat transfer equation. In cylindrical coordinates with a constant thermal conductivity, the two dimensional transient heat conduction equation can be written as:

$$\frac{\partial^2 T}{\partial r^2} + \frac{1}{r} \frac{\partial T}{\partial r} + \frac{\partial^2 T}{\partial z^2} + \frac{e_{\text{gen}}}{k} = \frac{1}{\alpha} \frac{\partial T}{\partial t} \quad 4-1$$

where T is temperature, r is the radial dimension, z is the axial dimension, e_{gen} is internal heat generation, k is thermal conductivity, α is thermal diffusivity and t is time.

The internal heat generation is proportional to the neutron flux, and the flux profile will vary throughout the core according to:

$$\text{Flux}(r) \propto J_0(\lambda r) \cos(Uz) \quad 4-2$$

Where λ is equal to $2.405/R$, U is π/H , R is the radius of the cylinder and H is the height.

Therefore 4-1 can be rewritten as:

$$\frac{\partial^2 T}{\partial r^2} + \frac{1}{r} \frac{\partial T}{\partial r} + \frac{\partial^2 T}{\partial z^2} + A J_0(\lambda r) \cos(Uz) = \frac{1}{\alpha} \frac{\partial T}{\partial t} \quad 4-3$$

In Equation 4-3, A includes k and other proportionality constants that will be looked at later.

The initial and boundary conditions will largely dictate if 4-3 is solvable. It is valid to assume that given enough time between runs the core initially will have reached thermal equilibrium at the surrounding ambient temperature T_{∞} . The initial condition is therefore:

$$T(r, z, 0) = T_{\infty} \quad 4-4$$

The symmetry of the problem yields the following conditions at $r = 0$ and $z = 0$.

$$\frac{\partial T(0, z, t)}{\partial r} = 0 \quad 4-5$$

$$\frac{\partial T(r, 0, t)}{\partial z} = 0 \quad 4-6$$

The boundary conditions at the outer edges of the core are the most difficult. Where two solid materials come together, the polyethylene core and the graphite reflector. For conduction between two solid materials at the radial boundary the following coupled equations apply:

$$T_c(R, z, t) = T_g(R, z, t) \quad 4-7$$

$$k_c \frac{\partial T_c}{\partial r} = k_g \frac{\partial T_g}{\partial r} \quad 4-8$$

The subscripts denote the core and the graphite respectively. Similar equations can be written for the axial outer boundary. This approach requires simultaneously solving multiple partial differential equations and is fairly complex. No analytic solution was found for this problem.

The problem can be simplified by assuming that at some point away from the core the thermal mass of the materials will be sufficiently large that the 5 watts of power generated from the reactor will have a negligible effect on temperature. In the radial direction the materials around the core can be considered to be concentric annuli. To get an idea of the temperature profile outside the core, the one dimensional steady state conduction equation can be solved for each solid cylindrical region. The equation is:

$$\frac{d^2 T_j}{dr^2} + \frac{1}{r} \frac{dT_j}{dr} = 0 \quad 4-9$$

where, the subscript j will be changed to g for graphite, l for lead, and s for steel. The boundary conditions for these equations are:

$$-k_g \frac{dT_g(R_{ig})}{dr} = q'' \quad 4-10$$

$$T_g(R_{og}) = T_l(R_{il}) \quad 4-11$$

$$k_g \frac{dT_g(R_{og})}{dr} = k_l \frac{dT_l(R_{il})}{dr} \quad 4-12$$

$$T_l(R_{ol}) = T_s(R_{is}) \quad 4-13$$

$$k_l \frac{dT_l(R_{ol})}{dr} = k_s \frac{dT_s(R_{is})}{dr} \quad 4-14$$

$$T_s(R_{os}) = T_\infty \quad 4-15$$

Here the assumption is made that infinite heat transfer takes place between the steel tank and the water. For clarity in the solution define $R_1=R_{ig}$, $R_2=R_{og}=R_{il}$, $R_3=R_{ol}=R_{is}$, $R_4=R_{os}$.

The solution to 4-9 is:

$$T_j(r) = C_{1j} \ln(r) + C_{2j} \quad 4-16$$

Applying the boundary conditions yields:

$$T_g(r) = R_1 q'' \left(\frac{\ln(R_2/r)}{k_g} + \frac{\ln(R_3/R_2)}{k_l} + \frac{\ln(R_4/R_3)}{k_s} \right) + T_\infty \quad 4-17$$

$$T_l(r) = R_1 q'' \left(\frac{\ln(R_3/r)}{k_l} + \frac{\ln(R_4/R_3)}{k_s} \right) + T_\infty \quad 4-18$$

$$T_s(r) = R_1 q'' \left(\frac{\ln \left(R_4 / r \right)}{k_s} \right) + T_\infty \quad 4-19$$

If no power is lost axially from the core then q'' is just the operating power divided by the surface area of the radial edge of the core. Figure 4-1 is the steady state change in radial temperature profile through the outer materials obtained from Equations 4-18 through 4-19 at 5 watts.

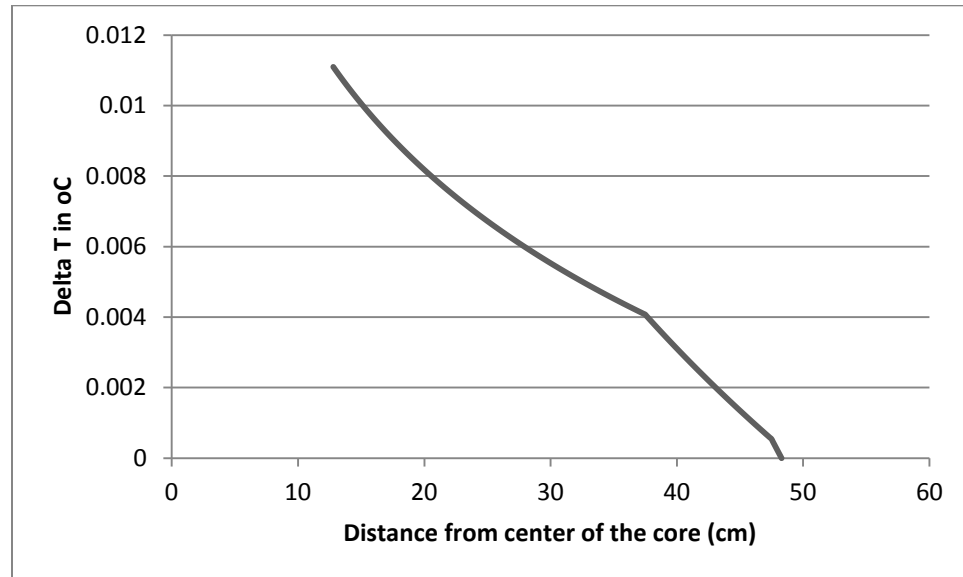


Figure 4-1 Temperature Change in Materials Outside the Core Operating at 5 W

From the graph it is seen that there is a negligible change in temperature from the edge of the core outward. Even at the low power the reactor operates at, an increase of 0.011 °C is insignificant. Therefore, it is valid to assume near infinite heat transfer at the core edge that will keep the edge temperatures at the ambient temperature. The final boundary conditions for the core are:

$$T(R, z, t) = T_\infty \quad 4-20$$

$$T(r, H/2, t) = T_{\infty} \quad 4-21$$

Equations 4-3 through 4-6 and 4-20 and 4-21 fully define the problem, but no method has been discovered to solve them in their current form. A variable substitution can be used to alter the equations to a solvable form. Assume that:

$$T(r, z, t) = \Theta(r, z, t) + C J_0(\lambda r) \cos(Uz) + T_{\infty} \quad 4-22$$

C is a constant used to remove the Bessel and cosine functions from the partial differential equation. The partial derivatives of T are therefore:

$$\frac{\partial T}{\partial r} = \frac{\partial \Theta}{\partial r} - C \lambda J_1(\lambda r) \cos(Uz) \quad 4-23$$

$$\frac{\partial^2 T}{\partial r^2} = \frac{\partial^2 \Theta}{\partial r^2} - C \lambda^2 J_0(\lambda r) \cos(Uz) + \frac{C \lambda}{r} J_1(\lambda r) \cos(Uz) \quad 4-24$$

$$\frac{\partial T}{\partial t} = \frac{\partial \Theta}{\partial t} \quad 4-25$$

$$\frac{\partial^2 T}{\partial z^2} = \frac{\partial^2 \Theta}{\partial z^2} - C U^2 J_0(\lambda r) \cos(Uz) \quad 4-26$$

Inserting 4-23 through 4-26 into 4-3 yields:

$$\begin{aligned} \frac{\partial^2 \Theta}{\partial r^2} - C \lambda^2 J_0(\lambda r) \cos(Uz) + \frac{1}{r} \frac{\partial \Theta}{\partial r} + \frac{\partial^2 \Theta}{\partial z^2} - C U^2 J_0(\lambda r) \cos(Uz) \\ + A J_0(\lambda r) \cos(Uz) = \frac{1}{\alpha} \frac{\partial \Theta}{\partial t} \end{aligned} \quad 4-27$$

If C is defined as:

$$C = \frac{A}{\lambda^2 + U^2} \quad 4-28$$

the Bessel and cosine terms will cancel out and the equation becomes the homogenous equation:

$$\frac{\partial^2 \Theta}{\partial r^2} + \frac{1}{r} \frac{\partial \Theta}{\partial r} + \frac{\partial^2 \Theta}{\partial z^2} = \frac{1}{\alpha} \frac{\partial \Theta}{\partial t} \quad 4-29$$

The initial and boundary conditions become:

$$\Theta(r, z, 0) = -\frac{A}{\lambda^2 + U^2} J_0(\lambda r) \cos(Uz) \quad 4-30$$

$$\frac{\partial \Theta(0, z, t)}{\partial r} = \frac{\lambda A}{\lambda^2 + U^2} J_1(0) \cos(Uz) = 0 \quad 4-31$$

$$\frac{\partial \Theta(r, 0, t)}{\partial r} = \frac{UA}{\lambda^2 + U^2} J_0(\lambda r) \sin(0) = 0 \quad 4-32$$

$$\Theta(R, z, t) = -\frac{A}{\lambda^2 + U^2} J_0(\lambda R) \cos(Uz) \quad 4-33$$

$$\Theta(r, H/2, t) = -\frac{A}{\lambda^2 + U^2} J_0(\lambda r) \cos(UH/2) \quad 4-34$$

To use the method of separation of variables Equations 4-33 and 4-34 need to be equal to 0. Note that the problem was defined using the bare cylindrical reactor assumption. Part of that assumption is that the flux is very near zero at the outer boundaries. Therefore it is in line with assumptions previously made to set 4-33 and 4-34 equal to 0.

The method of separation of variables assumes that Θ can be constructed as:

$$\Theta(r, z, t) = F(r)I(z)G(t) \quad 4-35$$

where F, I and G are single variable functions, of the radial, axial, and time variables.

Applying 4-35 to 4-29 yields the following ordinary differential equations:

$$\frac{d^2 F(r)}{dr^2} + \frac{1}{r} \frac{dF(r)}{dr} + B^2 F(r) = 0 \quad 4-36$$

$$\frac{d^2 I(z)}{dz^2} + D^2 I(z) = 0 \quad 4-37$$

$$\frac{dG(t)}{dt} + E^2 \alpha G(t) = 0 \quad 4-38$$

The constants in the above equations are related by:

$$E^2 = B^2 + D^2 \quad 4-39$$

The boundary conditions 4-31 through 4-34 are also separable and become:

$$\frac{dF(0)}{dr} = 0 \quad 4-40$$

$$F(R) = 0 \quad 4-41$$

$$\frac{dI(0)}{dz} = 0 \quad 4-42$$

$$I(H/2) = 0 \quad 4-43$$

4-36 is a form of Bessel's equation and has the solution:

$$F(r) = C_1 J_0(Br) + C_2 Y_0(Br) \quad 4-44$$

From boundary condition 4-40:

$$C_2 = 0 \quad 4-45$$

Boundary condition 4-41 yields:

$$C_1 J_0(BR) = 0 \quad 4-46$$

C_1 cannot be set to 0 without making entire solution the trivial solution. Therefore F becomes the series solution of eigenfunctions:

$$F(r) = \sum_{n=1}^{\infty} C_n J_0(B_n r) \quad 4-47$$

Where the values of the eigenvalues B_n are defined by:

$$J_0(B_n R) = 0 \quad 4-48$$

Note for the assumptions that have been made:

$$B_1 = \lambda \approx \frac{2.405}{R} \quad 4-49$$

The solution to 4-37 is:

$$I(z) = C_3 \cos(Dz) + C_4 \sin(Dz) \quad 4-50$$

The constants for the axial dimension work out the same way as the radial, 4-42 yields:

$$C_4 = 0 \quad 4-51$$

And 4-43 produces the series solution:

$$I(z) = \sum_{m=1}^{\infty} C_m \cos(D_m z) \quad 4-52$$

The eigenvalues are defined by:

$$\cos(D_m H/2) = 0 \quad 4-53$$

Similarly it is noted that:

$$D_1 = U = \frac{\pi}{H} \quad 4-54$$

The solution of 4-38 is:

$$G(t) = C_5 e^{-E_{nm}^2 \alpha t} \quad 4-55$$

The solution to Θ becomes:

$$\Theta(r, t) = \sum_{m=1}^{\infty} C_m \cos(D_m z) \sum_{n=1}^{\infty} C_n J_0(B_n r) e^{-E_{nm}^2 \alpha t} \quad 4-56$$

The constants C_n and C_5 have been combined in the above equation. Applying the initial condition, Equation 4-30, to 4-56 the following is obtained:

$$\sum_{m=1}^{\infty} C_m \cos(D_m z) \sum_{n=1}^{\infty} C_n J_0(B_n r) = -\frac{A}{\lambda^2} J_0(\lambda r) \cos(Uz) \quad 4-57$$

The Bessel eigenfunctions for this problem are orthogonal with respect to the weight function:

$$w(r) = r \quad 4-58$$

The values for C_n can be found by multiplying both sides of 4-57 by 4-58 and the eigenfunctions $J_0(B_p r)$ and integrating with respect to r from 0 to R .

$$\begin{aligned} \sum_{m=1}^{\infty} C_m \cos(D_m z) \sum_{n=1}^{\infty} C_n \int_0^R J_0(B_p r) J_0(B_n r) r dr \\ = -\frac{A}{\lambda^2} \cos(Uz) \int_0^R J_0(B_m r) J_0(\lambda r) r dr \end{aligned} \quad 4-59$$

Since they are orthogonal functions, over the interval, the integral on the left hand side of 4-59 is zero for any value of p except $p = n$. The equation then becomes:

$$\begin{aligned} \sum_{m=1}^{\infty} C_m \cos(D_m z) \sum_{n=1}^{\infty} C_n \int_0^R J_0^2(B_n r) r dr \\ = -\frac{A}{\lambda^2} \cos(Uz) \int_0^R J_0(B_n r) J_0(\lambda r) r dr \end{aligned} \quad 4-60$$

As indicated for Equation 4-49 λ , is an eigenvalue of this problem, therefore by the same logic the right hand side of 4-60 will be 0 for all values of B_n except $B_n = \lambda$. This results in all values of C_n except $C_{n=1}$ must be equal to 0. What is left is:

$$\sum_{m=1}^{\infty} C_m \cos(D_m z) C_{n=1} \int_0^R J_0^2(\lambda r) r dr = -\frac{A}{\lambda^2 + U^2} \cos(Uz) \int_0^R J_0^2(\lambda r) r dr \quad 4-61$$

The integrals in 4-61 cancel out and the equation becomes:

$$C_{n=1} \sum_{m=1}^{\infty} C_m \cos(D_m z) = -\frac{A}{\lambda^2 + U^2} \cos(Uz) \quad 4-62$$

The cosine eigenfunctions are orthogonal with a unity weight function over the interval $-H/2$ to $H/2$. Therefore, Equation 4-63 is obtained using 4-54 and the same technique employed on the Bessel eigenfunctions in 4-57 through 4-61.

$$C_{m=1}C_{n=1} \int_{-H/2}^{H/2} \cos^2(Uz)dz = -\frac{A}{\lambda^2 + U^2} \int_{-H/2}^{H/2} \cos^2(Uz)dz \quad 4-63$$

It is clear from 4-62 that:

$$C_{m=1}C_{n=1} = -\frac{A}{\lambda^2 + U^2} \quad 4-64$$

Again noting that all of the other C_m and C_n constants are equal to 0, $\Theta(r,z,t)$ is fully solved by substituting 4-64, 4-39, 4-49 and 4-54 into 4-56.

$$\Theta(r, z, t) = -\frac{A}{\lambda^2 + U^2} J_0(\lambda r) \cos(Uz) e^{-(\lambda^2 + U^2)\alpha t} \quad 4-65$$

The temperature profile is then constructed inserting 4-65 and 4-38 into 4-22.

$$\begin{aligned} T(r, z, t) = & -\frac{A}{\lambda^2 + U^2} J_0(\lambda r) \cos(Uz) e^{-(\lambda^2 + U^2)\alpha t} \\ & + \frac{A}{\lambda^2 + U^2} J_0(\lambda r) \cos(Uz) + T_\infty \end{aligned} \quad 4-66$$

This simplifies to:

$$T(r, z, t) = \frac{A}{\lambda^2 + U^2} J_0(\lambda r) \cos(Uz) (1 - e^{-(\lambda^2 + U^2)\alpha t}) + T_\infty \quad 4-67$$

Since the ambient temperature is arbitrary it is more useful to look at the change in temperature. In Equation 4-4 it is assumed that every point in the cylinder starts at the ambient temperature, therefore the change in temperature is simply:

$$\Delta T(r, z, t) = \frac{A}{\lambda^2 + U^2} J_0(\lambda r) \cos(Uz) (1 - e^{-(\lambda^2 + U^2)\alpha t}) \quad 4-68$$

4.2 Analysis of the Analytic Solution

Plotting Equation 4-68 with $z = 0$ yields Figure 4-2:

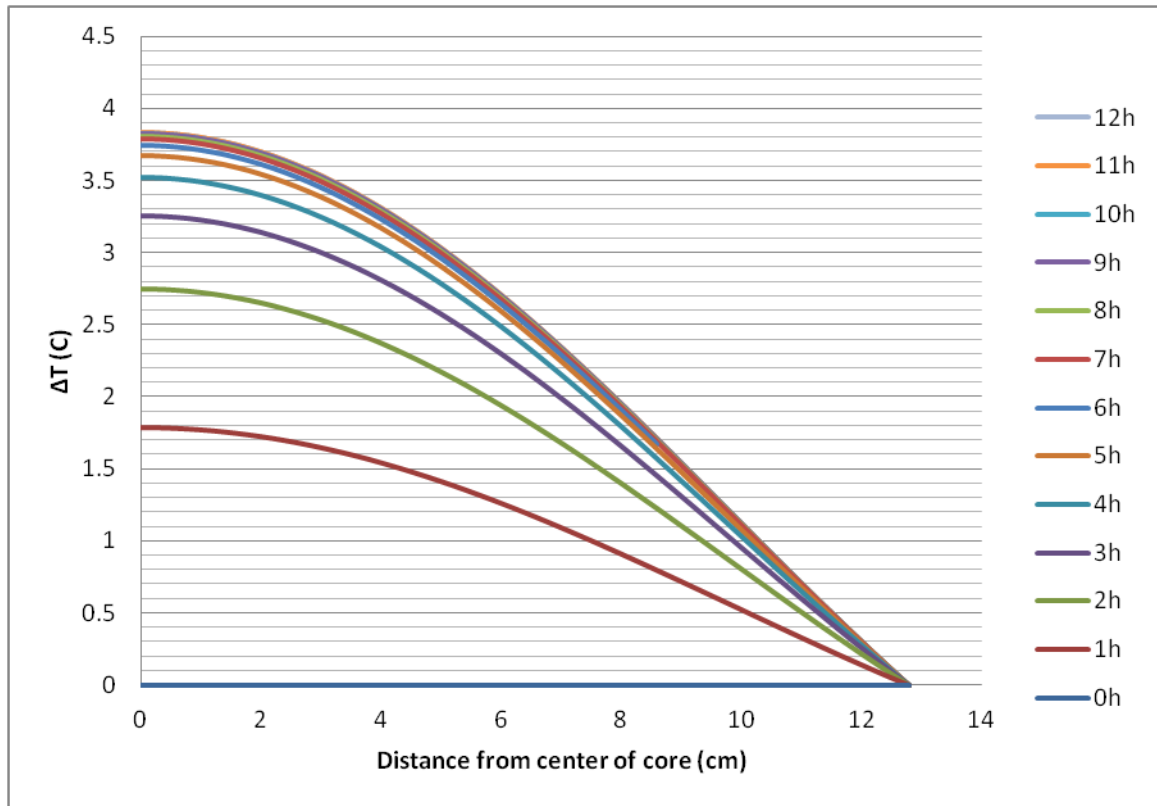


Figure 4-2 Plot of Analytic Solution

The Figure shows that the steady state conditions should be reached shortly beyond 12 hours.

The effectiveness of the analytic solution hinges on the homogeneous bare cylindrical reactor assumption. It is therefore worthwhile to look at how the assumed flux profile compares to the measured profile. A few different methods have been proposed to measure the flux profile in the AGN-201. (11) (2) An excerpt from the lab manual for the Idaho State University graduate reactor course explaining the procedure for the gold foil method is found in appendix C.

The experiment was performed by the author using 29 foils spaced 1 cm apart. As relative flux levels were the only things being looked at no effort was made to correct for detector efficiency to determine absolute flux. Also as most of the time the experiment is

performed only one cadmium ratio is found and then assumed constant for the entire reactor, that part of the procedure was also ignored and the thermal flux was assumed to be proportional to the total flux everywhere in the core.

Figure 4-3 is a plot of the determined flux profile with the center data point normalized to 1. The raw data can be found in appendix C.

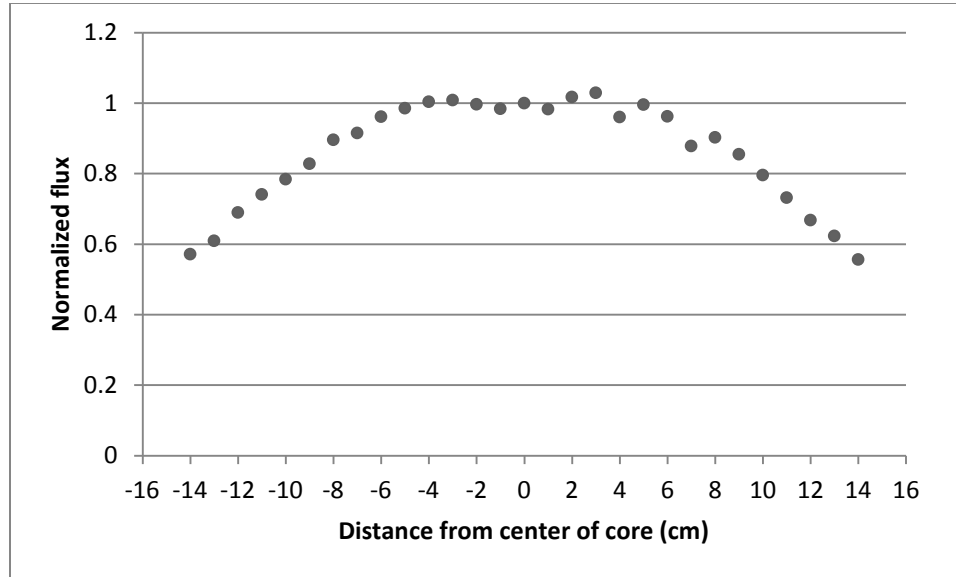


Figure 4-3 Normalized Flux Profile

Figure 4-4 is the same profile with the values for $J_0(\lambda r)$ added.

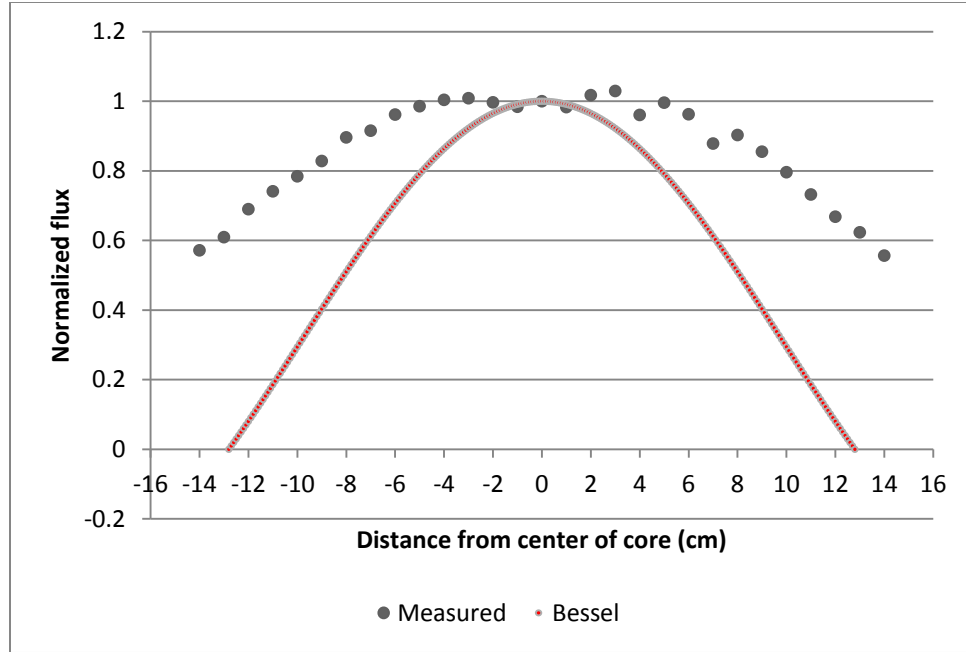


Figure 4-4 Flux Profile with Values for Bessel Function Added

The Bessel function does not match the measured data very well at all. A better normalization would have equal area under each curve, but because the curves represent a volume in space, equating the volumes found by rotating the curves around the z axis would be more accurate. Equation 4-69 does that:

$$\int_0^R J_0(\lambda r) r dr = D \int_0^R \text{flux}(r) r dr \quad 4-69$$

In the above equation D is the normalization value. The right hand side of 4-69 needed to be solved numerically. Simpson's rule was used to do so; the result is Figure 4-5.

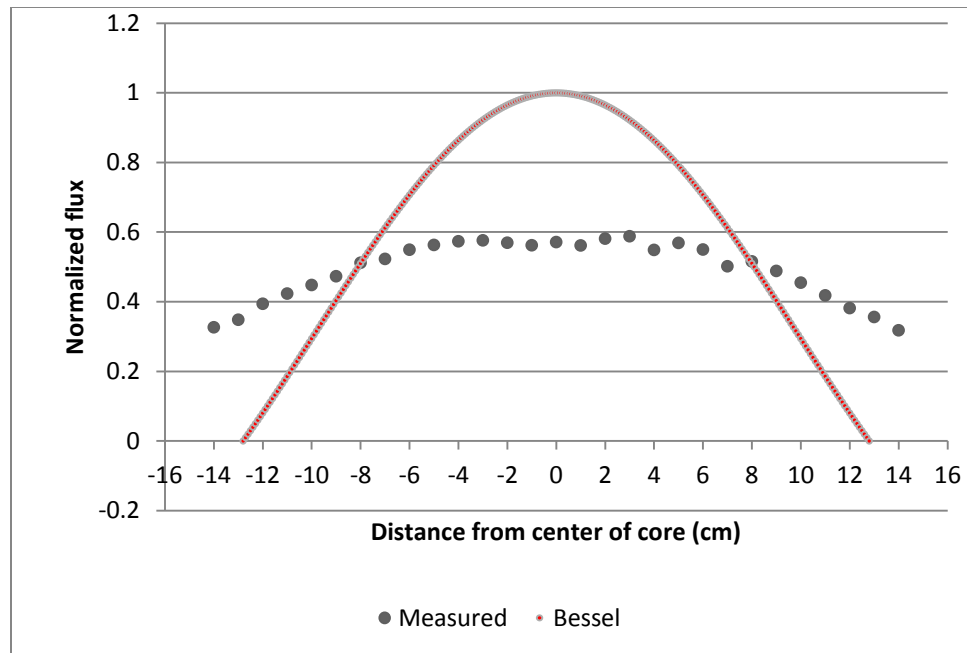


Figure 4-5 Measure and Assumed Flux Profiles, with Equal Volume Under the Curves

Figure 4-5 is an improvement, but it is still very clear that the flux does not vanish at the core boundary. To use the actual flux profile the equation must be solved numerically with a computer.

5 NUMERICAL SOLUTION

5.1 Formation

A numerical solution was developed by discretizing Equation 4-1. As change in temperature is more important than absolute temperature, the following variable substitution was used.

$$\theta(r, z, t) = T(r, z, t) - T_{\infty} \quad 5-1$$

Using second order central differences for the spatial terms and a first order rearward difference for the time term Equation 4-1 becomes:

$$\begin{aligned} \frac{\theta_{r+1,z,t} - 2\theta_{r,z,t} + \theta_{r-1,z,t}}{(\Delta r)^2} + \frac{1}{r} \frac{\theta_{r+1,z,t} - \theta_{r-1,z,t}}{2\Delta r} + \frac{\theta_{r,z+1,t} - 2\theta_{r,z,t} + \theta_{r,z,t-1}}{(\Delta z)^2} \\ + \frac{e_{\text{gen}}}{k} = \frac{1}{\alpha} \frac{\theta_{r,z,t} - \theta_{r,z,t-1}}{\Delta t} \end{aligned} \quad 5-2$$

The internal heat generation assumption used in Equation 4-2 could be used again, but as seen in the previous section the Bessel function approximation is not ideal. Instead, the data used to generate the flux profile in Figure 4-3 was used directly. Since no measurement of the axial flux profile can be made, the cosine assumption was still employed with zero flux boundary conditions at the axial edges of the core. The internal heat generation term therefore becomes:

$$\frac{e_{\text{gen}}}{k} = A \text{flux}(r) \cos(Uz) \quad 5-3$$

The constant A is found by integrating e_{gen} over the volume of the cylinder. Using $U = \pi/H$ where H is the height of the core A becomes:

$$A = \frac{P}{k4H \int_0^R \text{flux}(r) r dr} \quad 5-4$$

The integral in the denominator was evaluated numerically using the trapezoid rule. Additionally, a linear interpolation of flux(r) was used to determine its value at points in-between collected data points.

The axial symmetry boundary conditions are met by setting $\theta_{0,z-1,t}$ equal to $\theta_{0,z+1,t}$ for all values of z and t and $\theta_{r-1,0,t}$ equal to $\theta_{r+1,0,t}$ for all values of r and t. The infinite conduction boundary conditions are met by setting $\theta_{R,z,t}$ equal to 0 for all z and t, and $\theta_{r,Z,t}$ equal to 0 for all r and t. Initially all points are set to 0 at time $t = 0$.

Using these boundary conditions and Equation 5-2 a set of linear equations was developed for each time increment. The Matlab script labeled “Cylinder” in appendix D solves these equations. A uniform grid spacing of 0.2 cm was used throughout, with a time increment of 1 minute.

To determine when the time at which steady state is reached the steady state temperature is also calculated by removing the time component of 5-2. The code ceased when all points of the transient profile came within 0.001 of the steady state profile.

The core was also numerically modeled as an equivalent volume sphere. As the core radius is nearly equal to half the core height this assumption is fairly accurate. For a sphere, Equation 5-2 becomes:

$$\frac{\theta_{r+1,z,t} - 2\theta_{r,z,t} + \theta_{r-1,z,t}}{(\Delta r)^2} + \frac{2}{r} \frac{\theta_{r+1,z,t} - \theta_{r-1,z,t}}{2\Delta r} + \frac{e_{gen}}{k} = \frac{1}{\alpha} \frac{\theta_{r,z,t} - \theta_{r,z,t-1}}{\Delta t} \quad 5-5$$

The forcing function proportionality constant becomes:

$$A = \frac{P}{k4\pi \int_0^R \text{flux}(r)r^2 dr} \quad 5-6$$

The grid spacing was changed to 0.01 cm in the spherical case. The time increment and steady state criteria remained the same as in the cylindrical case. The spherical script is labeled Sphere in appendix D.

5.2 Analysis of Numerical Solution

Figure 5-1 is the steady state temperature distribution along the radial axis calculated using the cylindrical numeric model.

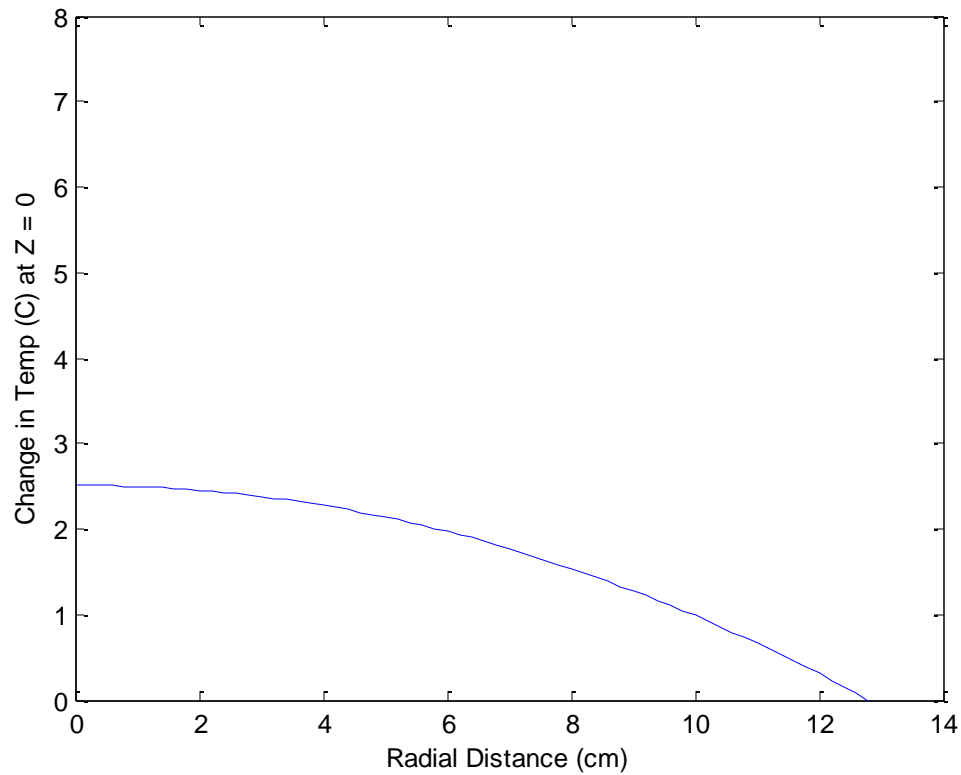


Figure 5-1 Steady State Radial Temperature Profile from Cylindrical Analysis, at $z = 0$

Figure 5-2 is the steady state temperature distribution along the radial axis using the spherical model.

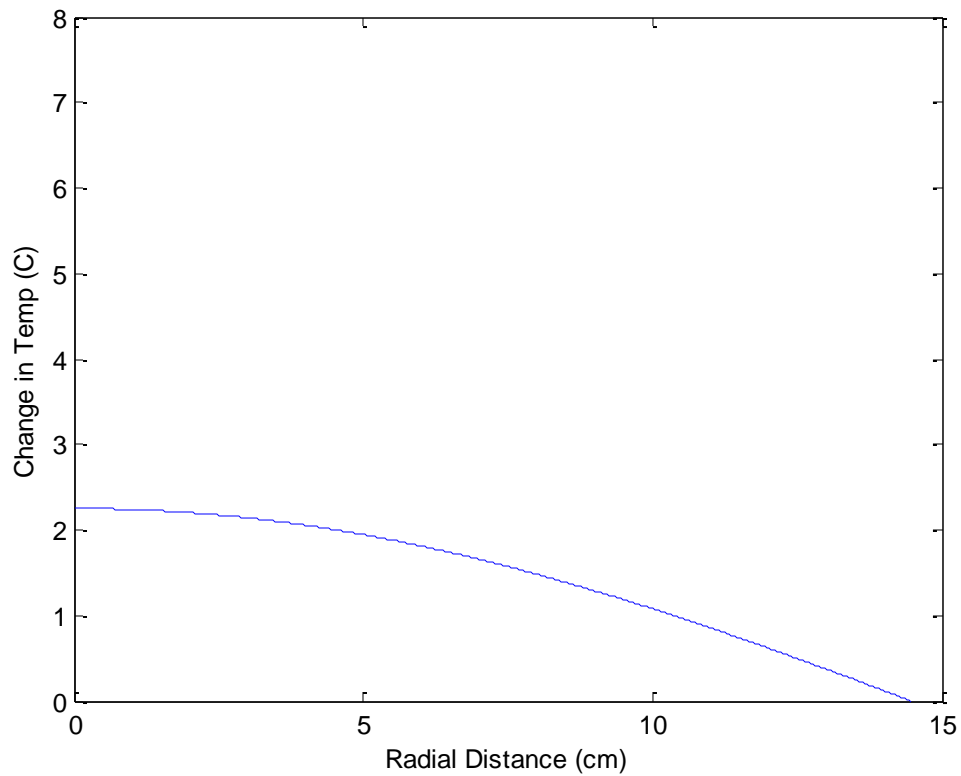


Figure 5-2 Steady State Temperature Profile from Spherical Analysis

The spherical model predicts slightly lower temperatures but is within 1 degree Celsius of the cylindrical model, which lends confidence to the assumption that the cylindrical core can be modeled as a sphere. The spherical model also benefits from not assuming that the flux goes to zero at any boundaries whereas the cylindrical model still assumes the flux is zero at the top and bottom of the cylinder.

6 CHANGE IN REACTIVITY WITH TEMPERATURE

The reactor physics code “Diffusion Iterative Solution for Nineteen Energy Groups” (DISNEL) was used to model and determine the k value of the reactor. Reference 12 describes how a DISNEL input deck is organized. (12) The input decks used for this project can be found in appendix E. The reactivity changes due to the following temperature effects were analyzed: 1) the change in the thermal utilization factor due to changes in the absorption cross sections; 2) change in the atom densities and dimension effects due to thermal expansion; 3) change in the resonance escape probability due to the “Doppler Effect;” and 4) change in the non-leakage probability.

Changing the temperature of the fuel materials in DISNEL was not able to fully account for all of these effects. Additional hand calculations were made to determine how either the DISNEL input deck or the k value output by DISNEL should be modified to include them.

6.1 Change in Thermal Utilization Factor

If the thermal cross sections of all the core atoms had exact $1/v$ dependence, the thermal utilization would not change with temperature. However, U-235 in particular has a cross section dependence at thermal energies which departs substantially from $1/v$ behavior. This departure is characterized by the “ g ” value shown in the following figure.

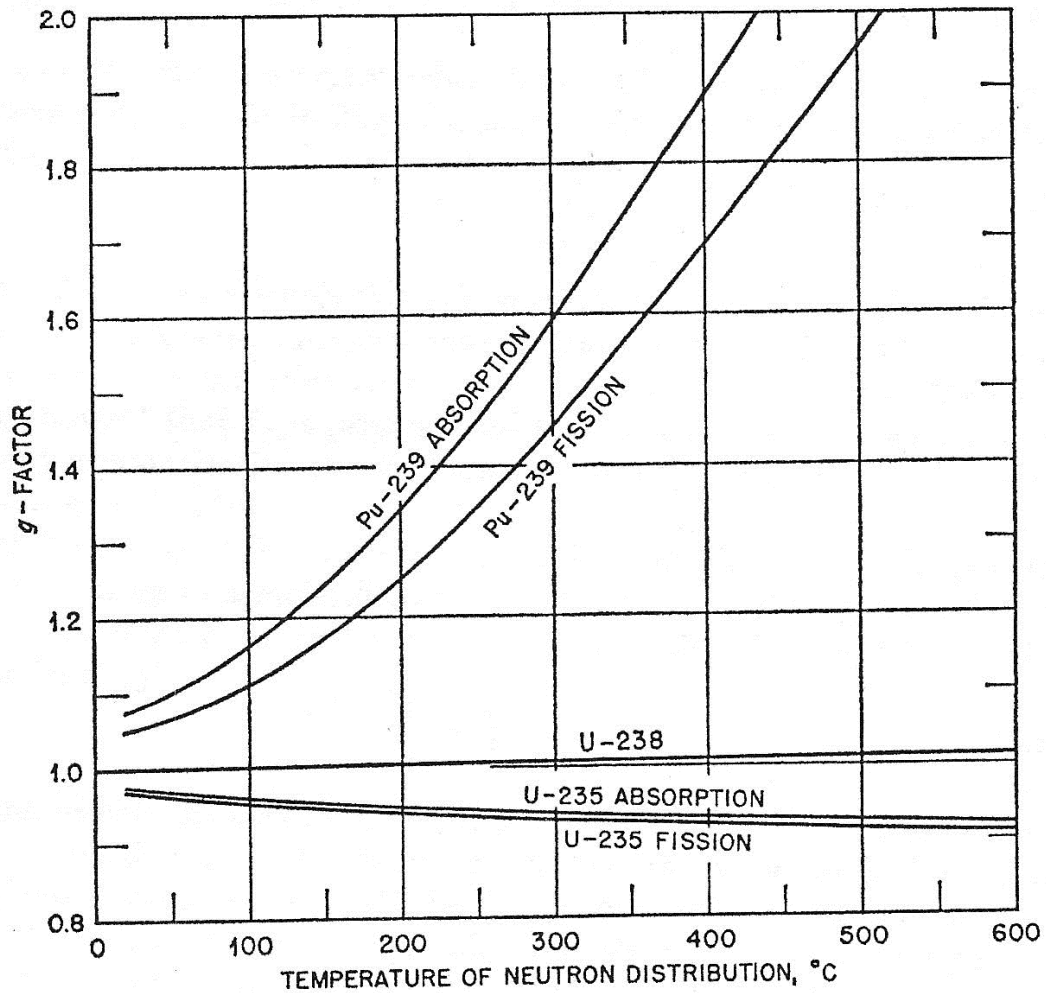


Figure 6-1 Values of g as a Function of Temperature (13)

The thermal utilization will decrease with increasing temperature because U-235 cross sections drop off faster than $1/v$, while hydrogen has a “g” factor that does not vary from 1.00. DISNEL has built in cross sections which take into account the change in the g-factor.

It should be noted that the thermal utilization and thermal non-leakage probability refer to thermal neutrons, or neutrons that have a Maxwell-Boltzmann energy distribution similar to their surrounding, and differs from the way the term thermal has been used up to this point. It does not reflect thermal energy being removed from the core.

6.2 Thermal Expansion

DISNEL does not inherently factor in thermal expansion. To account for this effect, changes to the atom densities and core geometry were calculated by hand and then modified in the input deck. The radial dimension in each region was changed according to the following equation:

$$R_{T2} = R_{T1}(1 + \Delta T \alpha) \quad 6-1$$

ΔT in 6-1 is the volume averaged change in temperature for the region. α is the linear expansion coefficient and has a value of $1.08 \times 10^{-5} / ^\circ\text{C}$ (13) for polyethylene. Similarly, the atom densities were reduced by:

$$N_{T2} = N_{T1}(1 - \Delta T \beta) \quad 6-2$$

β is the volume expansion coefficient and is approximated as 3α , which is a valid assumption for the relatively small temperature changes involved.

6.3 Doppler Effect

“Nuclei are located in atoms that are in continual motion owing to their thermal energy. As a result of these thermal motions, even a beam of strictly monoenergetic neutrons impinging on a target appears to the nuclei in the target as having a continuous spread in energy. This in turn, has an effect on the observed shape of a resonance. Thus, it can be shown that when the cross-section is averaged over the motions of the nuclei, the resonance becomes shorter and wider than when the nuclei are at rest. Furthermore, the effect becomes more pronounced as the temperature of the target goes up, as indicated in [Figure 6-2]. The change in shape of the resonance with temperature is called Doppler broadening.” (5)

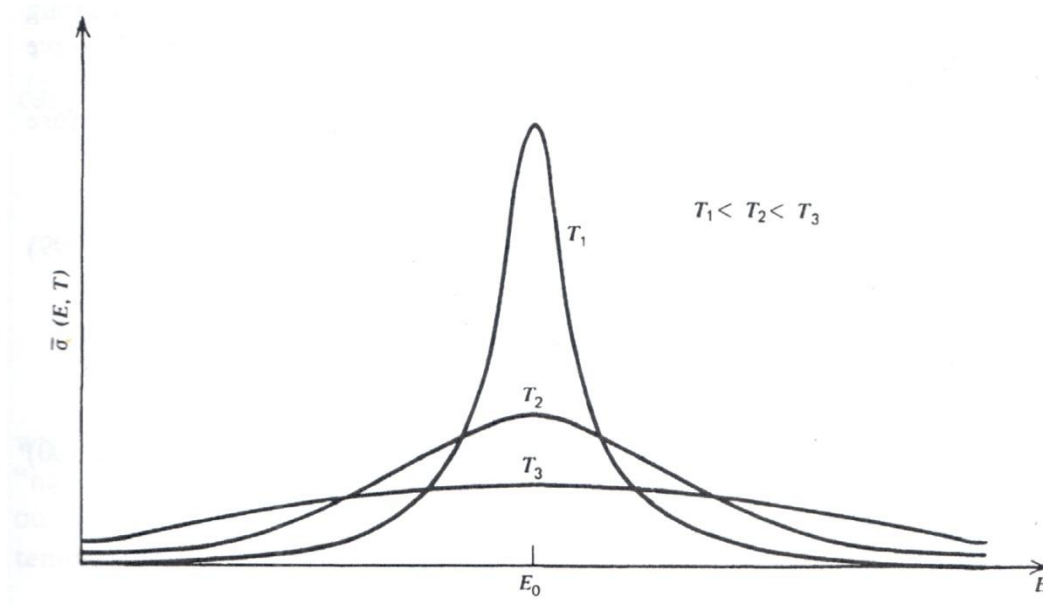


Figure 6-2 Doppler Broadening of Resonance with Increased Temperature (15)

“The broadened resonance increases the energy range over which absorption occurs. This effect outweighs the slight lowering of the resonance peak and gives rise to an enhanced absorption with increasing temperature.” (15) The net effect of Doppler broadening is a decrease of the resonance escape probability.

To account for the Doppler effect the correction factor for the 13th and 14th energy groups of the U-238 in the reactor were increased slightly.

6.4 Thermal Non-Leakage Probability

The change in the non-leakage probability is a result of thermal expansion. For reactors that are not moderated by hydrogen, the volume and density changes discussed in section 6-2 account for this effect. For hydrogen moderated reactors, additional hand calculations have to be made to account for the significant change in the scattering cross section of hydrogen as temperature increases as shown in Figure 6-3.

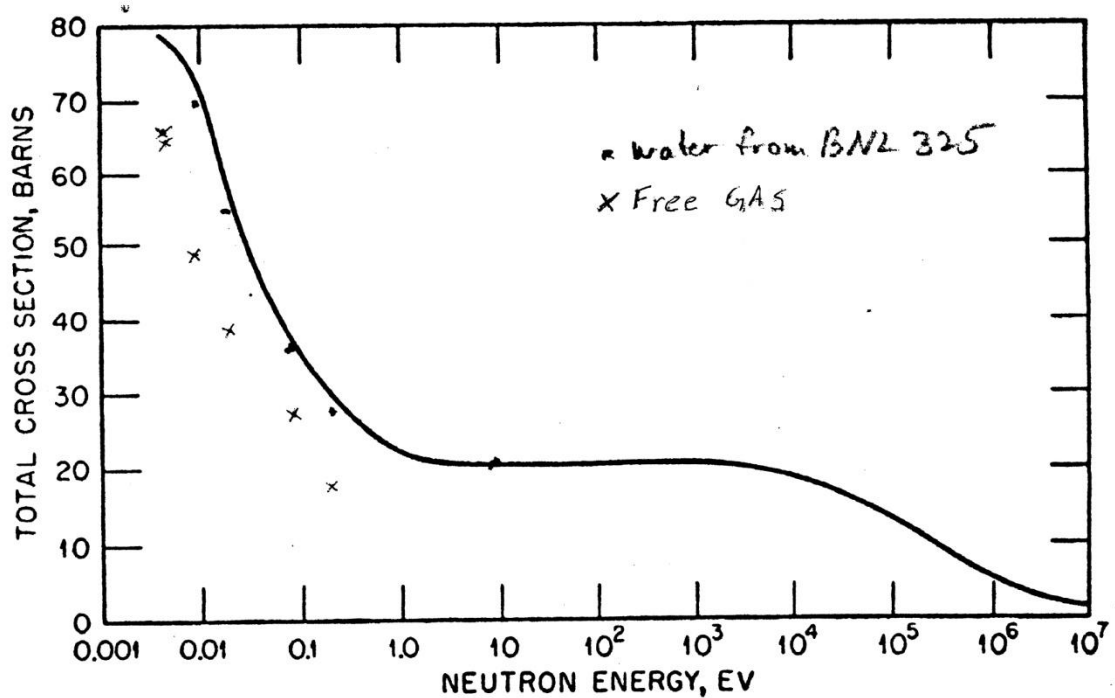


Figure 6-3 Cross Section of Hydrogen in Paraffin (16)

The curve on the Figure is for paraffin but also has data points taken from BNL 325 for free hydrogen gas and water. Since the cross sections of water line up with the cross sections of paraffin, it is assumed that the polyethylene cross sections will follow the same trend.

The microscopic scattering cross section of water is 103 barns. (5) Since the scattering cross section of carbon is 1 barn greater than that of oxygen, the scattering cross section of polyethylene was assumed to be 104 barns. The absorption cross section of water is 0.66 barns. The absorption cross sections of oxygen and carbon are much smaller than hydrogen therefore it was assumed the polyethylene the absorption cross section is the same as water.

The equation for the thermal non-leakage probability is:

$$NL_{th} = \frac{1}{1 + L^2 B^2} \quad 6-3$$

B^2 is π over the reflector savings radius of the core squared and was assumed to be constant. The reflector savings radius of the core was determined using DISNEL to find the radius of a bare core that had the same k as the reflected core and was found to be 19.09 cm. L^2 is the diffusion area and is defined for the moderator with the following:

$$L_{mod}^2 = \frac{1}{3\Sigma_{tr}\Sigma_a} \quad 6-4$$

The diffusion area for the core is:

$$L_{core}^2 = L_{mod}^2(1 - f) \quad 6-5$$

In Equation 6-5 f is the fuel utilization and is assumed to remain constant at 0.7 for this reactor. The transport cross section is:

$$\Sigma_{tr} = \Sigma_s(1 - \mu_0) \quad 6-6$$

μ_0 is the average scattering angle and is found by:

$$\mu_0 = \frac{2}{3A} \quad 6-7$$

A is the atomic weight of the polyethylene molecule approximately 14 amu.

6.5 DISNEL Validation

To validate the DISNEL plus hand calculation method, an initial input deck was constructed modeling the core as an equivalent volume sphere and dividing it into three concentric regions. The first region was the thermal fuse. The rest of the core was divided in half radially to form two additional regions. K was found for the case where all regions are at a uniform temperature of 68 °F to be 1.011304.

The DISNEL input deck was then modified to account for the aforementioned thermal effects and a uniform temperature rise of 40 °F yielding a k of 1.006668. That k

value was then modified by the ratio of the calculated non-leakage at 108 °F over the non-leakage at 68 °F.

$$\frac{NL_{th@108}}{NL_{th@68}} = \frac{0.97371}{0.97497} = 0.99871 \quad 6-8$$

The final k at 108 °F was found to be 1.005367 and the change in k to be -0.5937 %Δk/k, which is equivalent to -0.02671 %Δk/k per °C. This value falls in between the reported value of -0.025 and the value Mark Gaines determined of -0.03. It is therefore assumed the DISNEL plus hand calculation method adequately represents the temperature coefficient.

To quantify the contribution to the temperature coefficient of a single temperature effect, k was calculated using everything but that effect. This k was subtracted from the k of the combined temperature effects, 1.005367. The results are in Table 6-1.

Table 6-1 Reactivity Contribution of Individual Temperature Effects

Temperature Effect	K without effect	(%Δk/k per °C)	% Contribution
Thermal Utilization Factor	1.009015	-0.016416	61.53
Thermal Expansion	1.005576	-0.0009405	3.53
Self Shielding	1.006138	-0.0034695	13.00
Thermal Non-Leakage	1.006668	-0.0058545	21.94
Total		-0.0266805	100

6.6 Theoretical Reactivity Changes from Numeric Profiles

To determine the change in reactivity, it was necessary to create a unique DISNEL input file for each time step where the reactor core temperature profile had

changed. The initial k value was then subtracted from the k value generated at each time step.

It is not feasible to calculate the change in non-leakage or Doppler effect for the very small temperature changes in the core previously determined analytically and numerically. Therefore, it was assumed that the DISNEL output k would be decreased by a percentage proportional to the change that occurred in the 40 degree temperature change case. Equation 8-6 was used to determine the new k for each DISNEL output.

$$k_2 = k_{2DISNEL}(1 - 9.2596 * 10^{-5} \Delta T) \quad 6-9$$

The value $9.2596 * 10^{-5}$ was determined using the 40 degree delta T case. Equation 6-9 can only apply to the entire core and not different temperature regions. The delta T used must therefore be the volume averaged delta T for the core. Therefore, the effect of using the volume averaged core temperature versus a temperature profile needed to be addressed.

To model the temperature distribution in DISNEL, the core was modeled using discrete temperature regions. In each region the spherical numeric temperature profile was used, along with the Matlab code labeled “AverageTemps” to calculate the volume averaged temperature for that region.

The numerical temperature profile at the time $t = 400$ minutes was used to develop DISNEL inputs with 1 through 5 regions. The output k values are shown in Table 6-2.

Table 6-2 Comparison of k with Number of Temperature Regions

Number of Regions	K
1	1.011169

2	1.011169
3	1.011165
4	1.011166
5	1.011167

The table shows that increasing the number of temperature regions produces a negligible change in k at a 2°C temperature change. To simplify the analysis when calculating k for the other time steps only 2 regions were used, the thermal fuse and a large outer region both at the average temperature. The calculated average core temperatures for each time step are in Table 6-3.

Table 6-3 Calculated Average Core Temperatures for Each Time Step

Time (min)	Average Core Temp ($^{\circ}\text{F}$)
0	68.000000
100	68.941940
200	69.282860
300	69.416600
400	69.469160
500	69.490040
600	69.498140
700	69.501380
757	69.502280

A lack of change in the k value as the number of temperature regions increases indicates that the isothermal temperature coefficient is the same as the dynamic

temperature coefficient. It was of interest to check if this remains true for temperature profiles that have a maximum temperature greater than a few degrees. To do so the spherical numeric code was used to determine the steady state profile at 100 watts. Figure 6-4 is the profile.

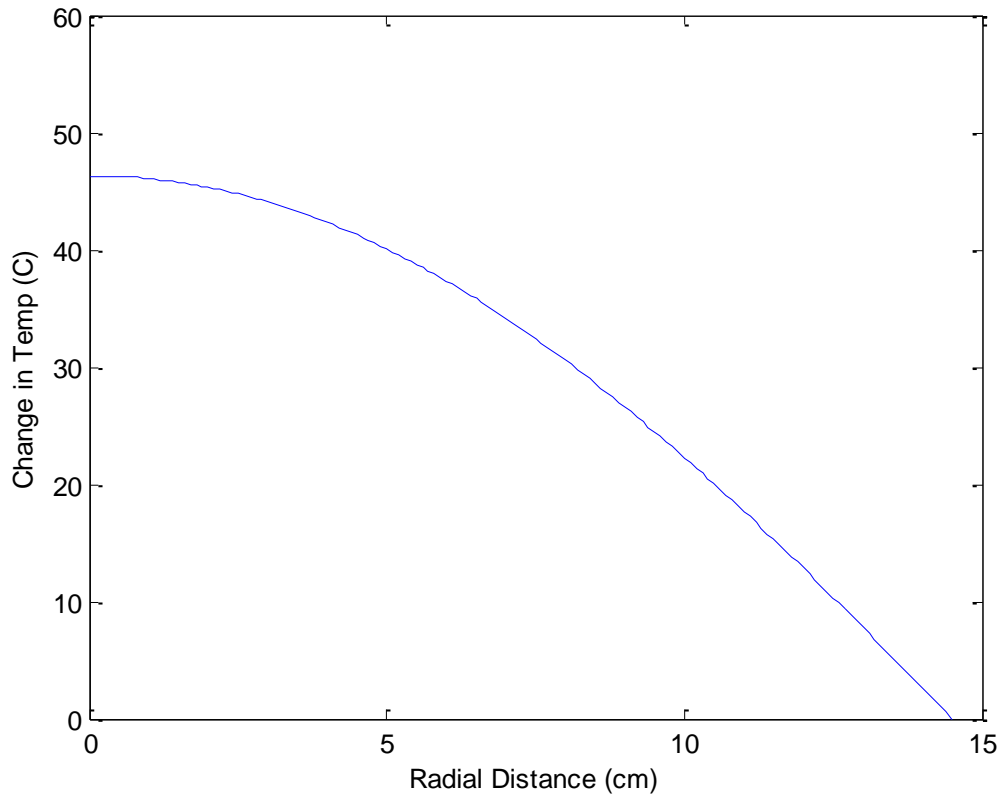


Figure 6-4 100W Steady State Temperature Profile

DISNEL input decks were created using 2 regions at the volume averaged temperature of the core and 5 regions at different volume averaged temperatures. The 2 region k was 1.008336 while the 5 region k was 1.008490. Clearly there is a difference between the temperature coefficients at larger temperature differences.

7 EXPERIMENT

7.1 Initial Experiment

An initial experiment was performed prior to the start of this project to determine if the reactivity change due to temperature was of sufficient magnitude to further investigate. The reactor was brought up to a power level of approximately 3.74 watts (2.6×10^{-7} amps on channel 3). In order to hold the power constant, the reactor operator watched the indicator on channel 3 and would periodically insert more of the fine control rod to compensate for drift in the power as the core heated up. This was done for 110 minutes, after which the fine control rod was returned to its original position putting the reactor on a negative period. Inverse kinetics was used to analyze power data collected by the laboratory data acquisition system and determine the difference in reactivity between the two critical rod heights. The result was a change of $-0.0121 \text{ \%}\Delta k/k$.

7.2 Temperature and Reactivity Measuring Experiment

The polyethylene core is contained within an air-tight aluminum tank. There is not a practical way to run instrumentation through the core tank while remaining compliant with facility regulations. Therefore, a direct measurement of the core temperature is not possible. The closest a temperature probe can get to the core is from within the glory hole. Figure 7-1 is the device that was built to hold thermocouples at a fixed location within the glory hole.

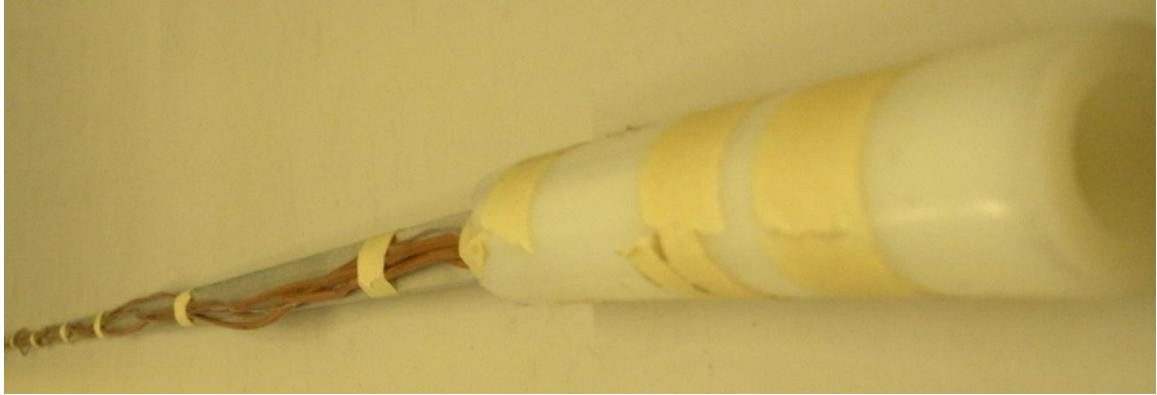


Figure 7-1 Core Temperature Measuring Device

The device consists of a flat aluminum rod attached to a hollow polyethylene tube. Four thermocouples were attached to the outside of the polyethylene as can be seen in Figure 7-2.



Figure 7-2 Thermocouples on the Polyethylene Tube

The rod is of a sufficient diameter to push the thermocouple firmly against the inner edge of the glory hole. The thermocouple beads are taped into place. The rest of the thermocouple wire is run through a hole in the polyethylene tube and out the back, taped to the aluminum rod. The aluminum rod was marked in such a way that when inserted the thermocouples would start 1 inch from the center of the core and continue out every

inch for 4 inches. The thermocouples are connected to a thermocouple reader (make and model number) shown in Figure 7-3.



Figure 7-3 Thermocouple Reader

The reader sampled and recorded the thermocouple temperatures every 10 seconds.

The reactor was brought to a power of 4.9 watts ($\sim 3.4 \times 10^{-7}$ amps on channel 3). The power was held constant with the closed loop oscillator. The closed loop oscillator was attached to a Labview program designed to record time, reactor power and oscillator rod position. A small piece of cadmium is affixed to the oscillator rod. The Labview program holds the reactor power constant by moving the cadmium piece toward or away from the core whenever changes in power are detected. The reactivity worth of the

oscillator rod was calculated by Tony Riley in his master thesis (17) and corresponds to the Equation (17):

$$\rho = 3.89E^{-2} - 3.46E^{-3}x + 8.25E^{-5}x^2 \quad 7-1$$

where ρ is reactivity in $\% \Delta k/k$ and x is centimeters from an imaginary plane running through the center of the core perpendicular to the oscillator rod. Equation 7-1 gives absolute reactivity, whereas the value of interest is the change in reactivity. Therefore x_0 is defined as the starting position of the rod when the reactor was brought to power and the change in reactivity is calculated using Equation 7-2.

$$\Delta\rho = 3.46E^{-3}(x_0 - x) + 8.25E^{-5}(x^2 - x_0^2) \quad 7-2$$

The reactor remained at power for 417 minutes. About 280 minutes into the experiment the recording device was bumped and the reading on thermocouple 1 instantly raised about 2 degrees. At 292 minutes into the experiment the oscillator rod was close to running out of range. At that point the Fine Control Rod on the reactor console was inserted 1.20 cm to move the oscillator rod in closer to the core. From that point on Equation 7-2 was adjusted by adding 0.0246 $\% \Delta k/k$ of reactivity. The experiment was ended when it appeared that the temperature was no longer changing.

7.3 Experimental Results

Figure 7-4 plots the change in temperature over time for all four thermocouples.

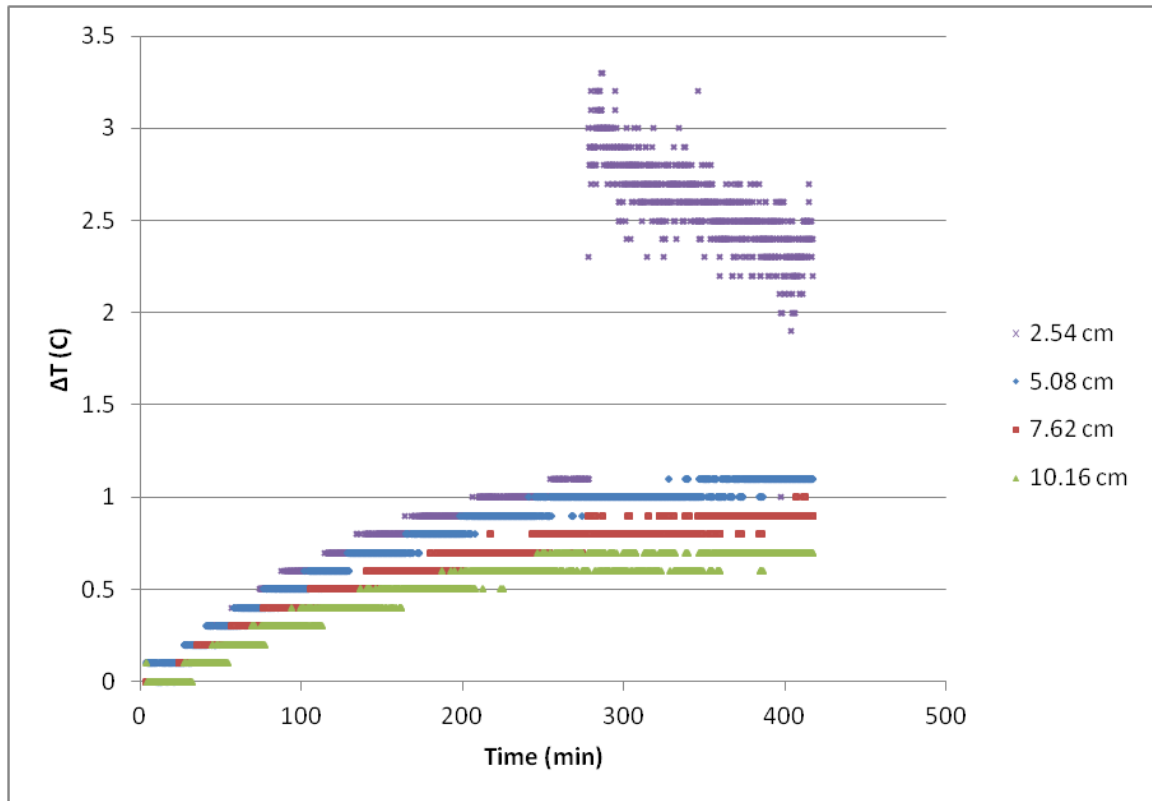


Figure 7-4 Recorded Change in Temperatures for all Thermocouples

It is clear from 7-4 that the 2.54 cm thermocouple was affected when the thermocouple reader was bumped. Therefore that data will not be included in the rest of the results and analysis. Figure 7-5 is the same as 7-4 but without the 2.54 cm data.

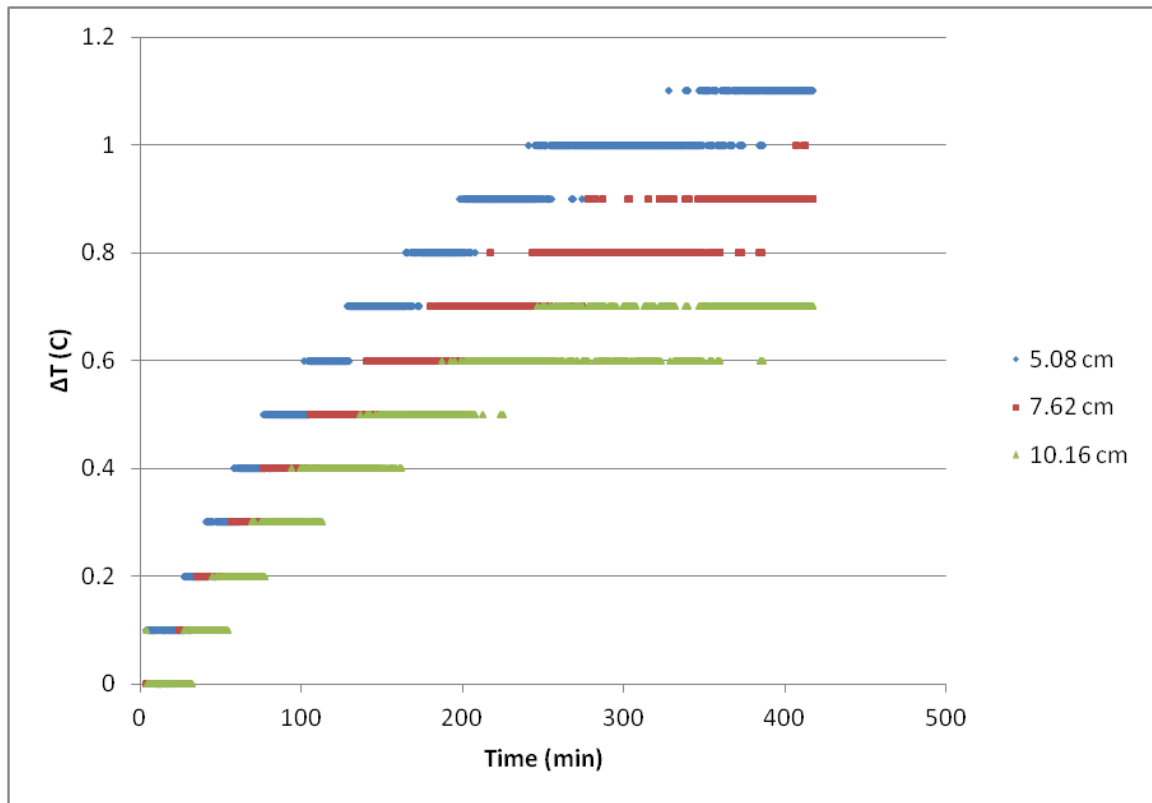


Figure 7-5 Recorded Change in Temperatures for Thermocouples Excluding 2.54 cm

Using Equation 7-2 to convert the oscillator rod position into reactivity insertion over time yields Figure 7-6.

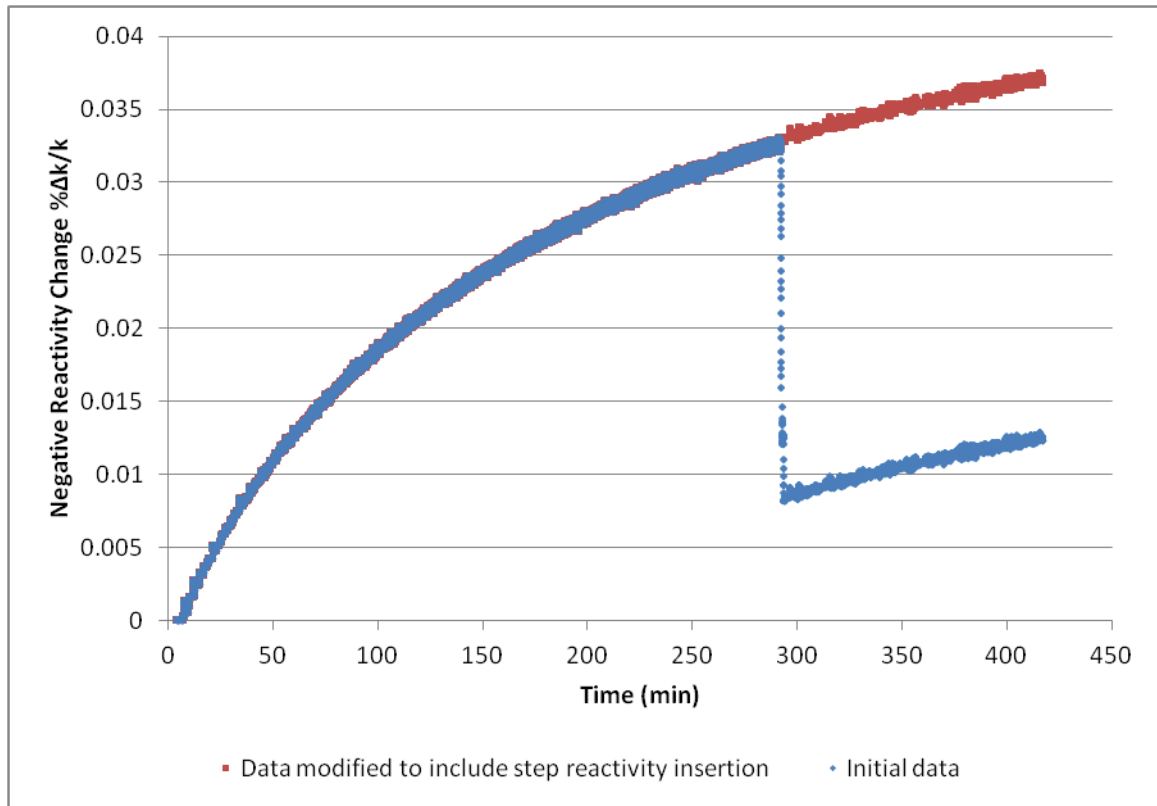


Figure 7-6 Measured Reactivity Insertion vs Time

The point at which the fine control position was changed can clearly be seen on the figure. The blue line shows the oscillator removing reactivity to compensate for the reactivity added by the fine control rod. Net reactivity insertion was calculated by adding the value of the FCR reactivity insertion (0.0246 %Δk/k) to the oscillator rod insertion data after the 292 minute mark.

It is clear from plots 7-5 and 7-6 that the temperature of the reactor had not reached steady state by the time the experiment was concluded.

8 COMBINED RESULTS AND ANALYSIS

Figure 8-1 compares the various temperature profiles at 417 minutes. The line labeled analytic is the derived solution from Equation 4-68 with $z=0$. The lines labeled cylinder and sphere are the numerical solutions from section 5. The cylinder is using the data at $z=0$. The line labeled measured is the data from the three working thermocouples from the experiment.

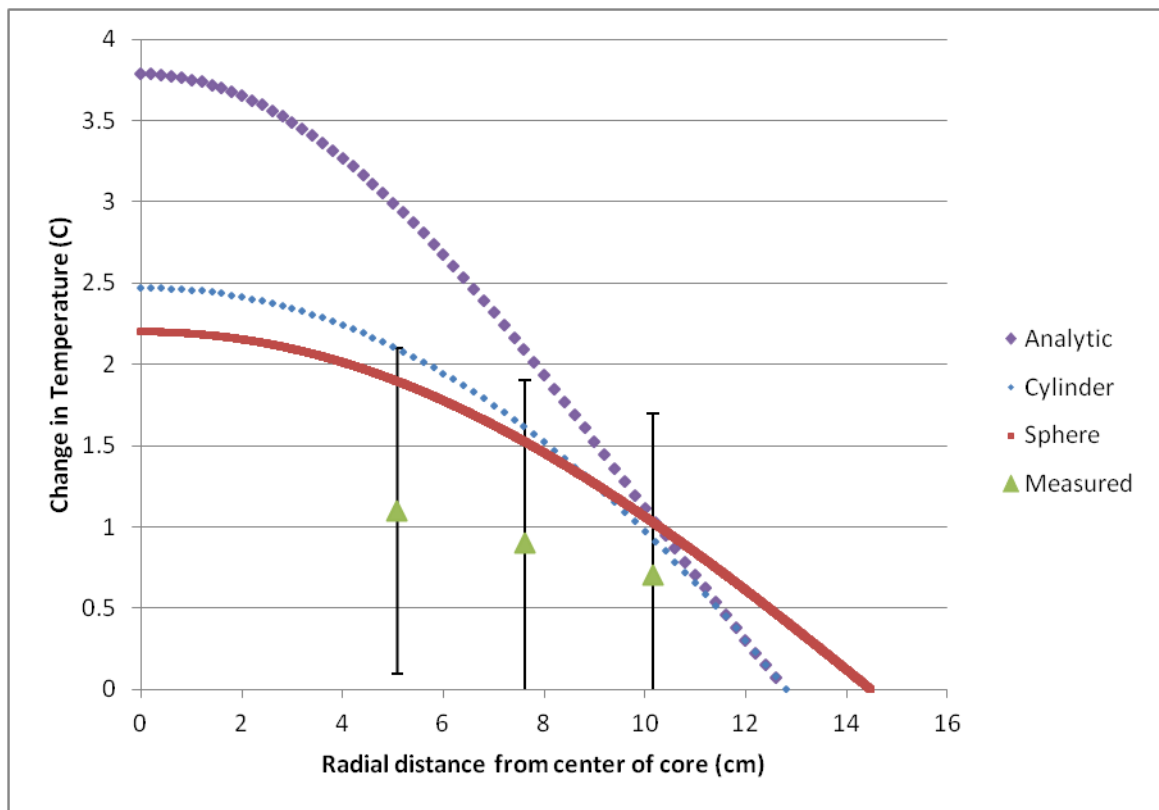


Figure 8-1 Temperature Profiles at 417 Minutes

The analytical solution predicts the greatest maximum temperature with the sharpest slopes. The measured temperatures show a much more gradual slope than any of the theoretical solutions. While the numerical spherical approach is the closest to matching the experimental data all theoretical curves indicate greater temperatures than

measured. The analytic curve is the only one that predicts values outside the error bars of the measured values.

Figure 8-2 compares the calculated temperature at 5.08 cm out from the center of the core to the measured value.

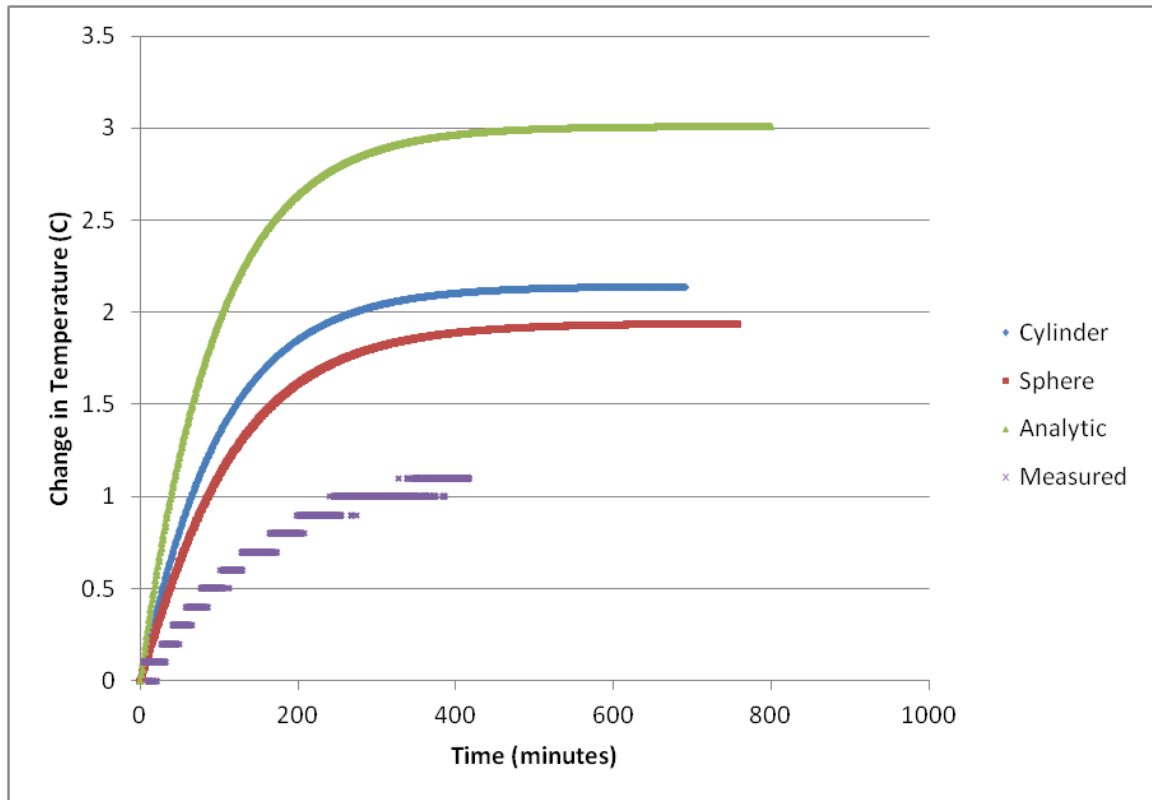


Figure 8-2 Change in Temperature at 5.08 cm Radially

Figure 8-3 compares the theoretical reactivity change calculated using DISNEL and the numerical spherical temperature profile (procedure in section 6.6) with the measured reactivity change from the experiment.

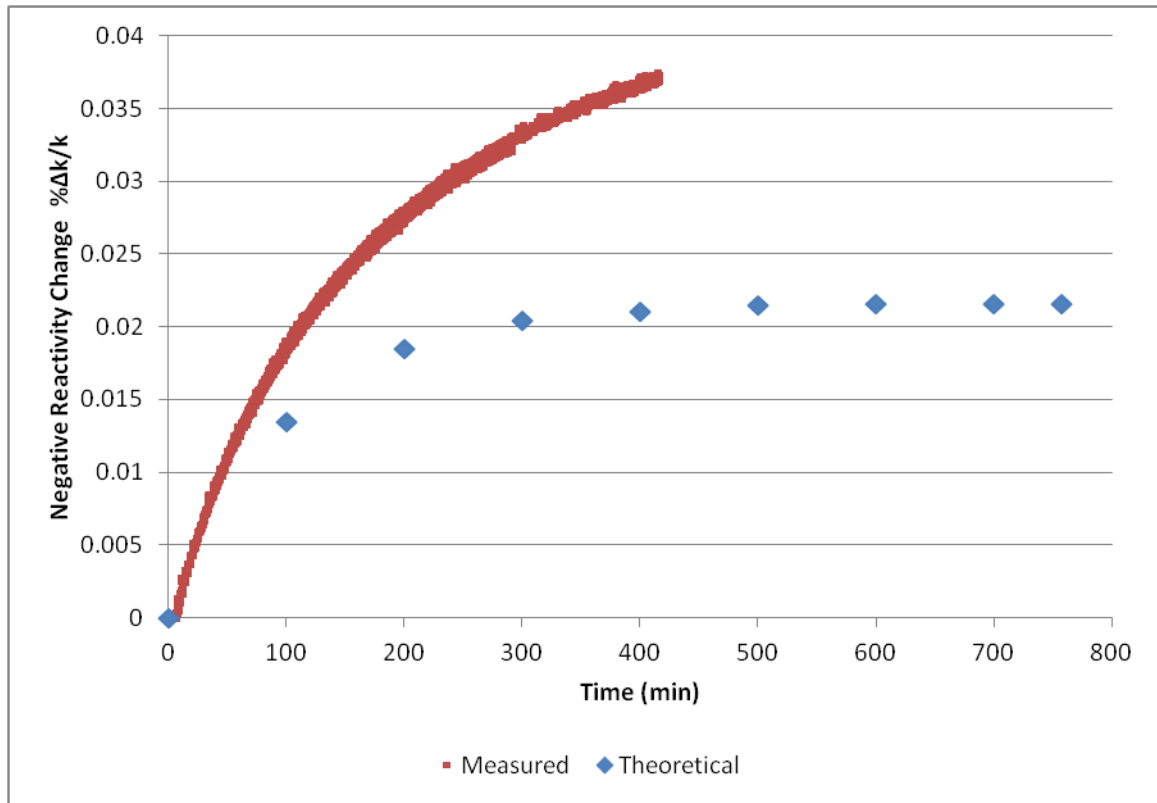


Figure 8-3 Measured and Theoretical Reactivity Insertion vs Time

It is strange that the theoretical reactivity insertion is lower than the experimental. The higher change in reactivity suggests that the actual temperature of the core is higher than the theory indicates. However, Figure 8-1 clearly shows the measured temperature to be lower than the theoretical temperature. The only way to rectify this would be to increase the multiplier used to correct the DISNEL solutions. As this multiplier has already been shown to predict the uniform temperature coefficient within 10%, it is assumed it is not the source of the error.

Since the average temperature is all that is necessary to determine change in reactivity, it is possible to develop an empirical formula for the reactivity insertion as a function of reactor power level and time. From Figure 8-2 it can be seen that although the analytic solution is the furthest off, the form of the curve does match the experimental

results. Therefore, the empirical formula should be in the form of Equation 4-68 without any spatial dimensions as shown in Equation 8-1.

$$\Delta\rho(P, t) = MP(1 - e^{-Lt}) \quad 8-1$$

Curve fitting the measured reactivity insertion data yields an M value of 0.0080327 % $\Delta k/k/W$ and L is equal to 0.0061499 /min. Figure 8-4 compares this curve fit with the measured data.

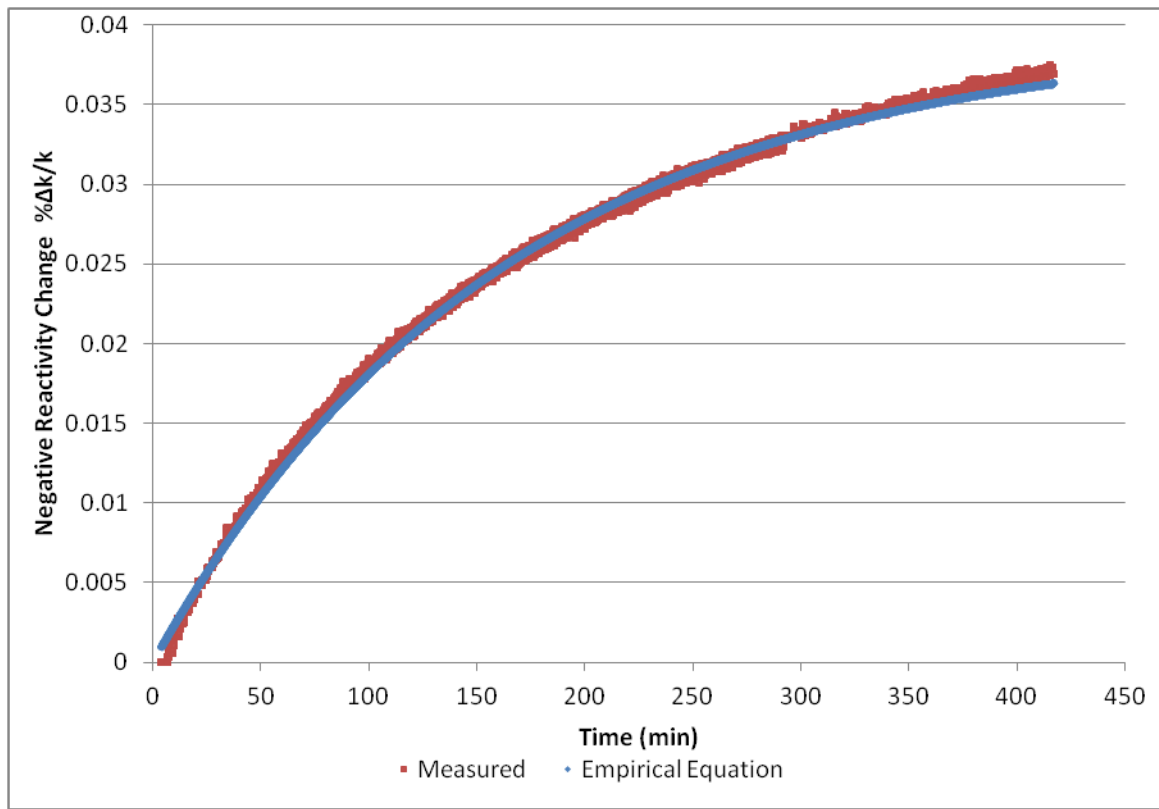


Figure 8-4 Measured and Empirical Reactivity Insertions

The data from the initial temperature experiment can be used to further test the empirical solution. Using 3.74 watts and 110 minutes in Equation 8-1 yields 0.0153 % $\Delta k/k$, whereas 0.0121 % $\Delta k/k$ was measured or a 26.4% difference.

9 CONCLUSION

All attempts to model the reactor temperature profile either analytically or numerically produced significantly higher results than were measured. The numerical results fell within the upper bounds of the measurement error. The analytical result did not. The temperature measuring device constructed was not able to accurately measure the core material temperature.

Even though the DISNEL plus hand calculation method predicted the measured temperature coefficient within 10%, using the method with a numeric temperature profile to determine the change in reactivity in the core with time produced low results.

Using the measured reactivity change in the core to develop an empirical solution of the form of the analytical results produced a curve fit that can be used for other temperature applications.

The coefficient of reactivity was calculated to be $-0.02671 \text{ } \Delta k/k \text{ per } ^\circ\text{C}$. The primary temperature feedback mechanism for the reactor comes from the change in thermal utilization.

The dynamic and isothermal temperature coefficients diverge as the temperature of the core increases, particularly so under rapid dynamic increase in power.

REFERENCES

1. **Harris, Shelbie.** 50 Years and Still Young: ISU Celebrates Golden Anniversary of Reactor. [Online] Idaho State University, 2015. [Cited: November 24, 2015.] <http://isubengal.com/50-years-and-still-young-isu-celebrates-golden-anniversary-of-reactor/>.
2. **Gorham, Mackenzie L.** *Experimantal Paramaterization of the Idaho State University AGN-201 Research and Training Reactor*. Pocatello, ID : Idaho State University, 2012.
3. **Baker, Benjamin A.** *Reactor Parameter for the ISU-AGN-201 Reactor*. Pocatello, ID : Idaho State University, 2011.
4. —. *Comparison of Open Loop and Closed Loop Reactivity Measurement Techniques on the ISU-AGN-201 Reactor*. Pocatello, ID : Idaho State University, 2013.
5. **Lamarsh, John R. and J., Baratta Anthony.** *Introduction to Nuclear Engineering*. Upper Saddle River, NJ : Prentice Hall, 2001. p. 367.
6. —. *Safety Analysis Report of the Idaho State University AGN-201 M Research Reactor*. Pocatello : Idaho State University, 2003.
7. **Ruzich, K. C. and J., Strum W.** *Hazard Summary Report For The Argonne AGN-201 Reactor*. Argonne, IL : Argonne National Laboratory, 1962.
8. **Gaines, Mark.** *Reactor Temperature Coefficient*. Pocatello, ID : s.n., 2010.
9. **Popov, S. G., et al.** *Thermophysical Properties of MOX and UO2 Fuels Includeing the Effects of Irradiation*. Oak Ridge : Oak Ridge National Laboratory, 2000.
10. **INEOS Olefins & Polymers USA.** *Typical Engineering Properties of High Density Polyethylene*. League City : www.ineos-op.com, 2009.
11. **Baker, Benjamin.** *Nuclear Reactor Lab Manual*. Pocatello, ID : Idaho State University Nuclear Engineering Department, Idaho State University Nuclear Engineering Department, 2014.
12. **Byambadorj, Bilguun.** *Upgrade of a Deterministic Multi-Energy Group Diffusion Reactor Physics Code*. Pocatello : Idaho State University, 2014.
13. **Gladstone, Samuel: Sesonske, Alexander.** *Nuclear Reactor Engineering*. s.l. : Van Nostrand, 1963.
15. **Duderstadt, James J. and Hamilton, Louis J.** *Nuclear Reactor Analysis*. s.l. : John Wiley & Sons, Inc, 1976. pp. 49, 337.
16. **Glasstone, Samuel and Edlund, Milton C.** *The Elements of Nuclear Reactor Theory*. New York, NY : D. Van Nostrand, 1952.

17. **Riley, Tony.** *Calibration of Reactivity Oscillator for ISU-AGN-201 Reactor.* Pocatello, ID : Idaho State University, 2013.

APPENDIX A – MARK GAINES REPORT

8/9/2010

Memo: Reactor Temperature Coefficient

From: Mark Gaines

To: Dr. Jay Kunze & Adam Mallicoat

Previously the temperature coefficient used to estimate excess reactivity (from which rod heights at criticality are derived) was -0.02% Delta K/K per degree Celsius increase in tank water temperature. Based on the data in Fig 1, taken from every run that reached critical since Jan 20, 2009, it would be more accurate to use a coefficient of -0.03% Delta K/K per degree Celsius increase in tank water temperature.

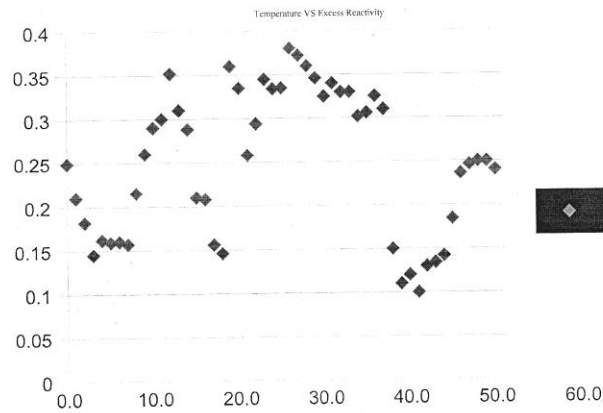


Fig. 1. Linear Approximation of AGN temperature coefficient.

Table 1. Run data from Master Log

Date	Temp °C	Excess Reactivity (%Delta K/K)
1/6/2010	19	0.249
1/7/2010	19.9	0.21
1/8/2010	21	0.182
1/10/2010	22.5	0.145
1/12/2010	22.9	0.162
1/13/2010	22.5	0.159
1/13/2010	22.5	0.16
1/14/2010	22	0.157
1/20/2010	20	0.215
2/4/2010	20	0.26
3/31/2010	16	0.29
4/7/2010	15.5	0.3
4/14/2010	16.2	0.352
4/16/2010	17	0.31
4/21/2010	18	0.288
6/29/2010	20.75	0.21
7/9/2010	20.5	0.208
7/20/2010	23	0.156
8/3/2010	23.5	0.146
1/20/2009	16.2	0.36
2/10/2009	17.5	0.335
2/25/2009	20	0.258
3/4/2009	18.5	0.294
3/30/2009	16.3	0.345
3/31/2009	17	0.334
4/1/2009	17	0.335
4/3/2009	16.2	0.38
4/8/2009	16	0.372
4/17/2009	16.1	0.36
4/21/2009	16.8	0.346
4/22/2009	17	0.325
4/22/2009	17.3	0.34
4/23/2009	17.8	0.33
4/23/2009	17.8	0.33
6/9/2009	19	0.302
6/12/2009	18.7	0.306

6/19/2009	18	0.325
6/22/2009	18.3	0.31
7/21/2009	22.8	0.15
7/27/2009	23.5	0.11
7/28/2009	23.5	0.12
8/7/2009	23.5	0.1
8/10/2009	22.3	0.13
9/2/2009	22.5	0.134
9/21/2009	22.1	0.142
10/5/2009	20	0.184
10/12/2009		
9	18.5	0.236
10/26/2009		
9	18.2	0.246
10/28/2009		
9	18	0.25
12/15/2009		
9	18	0.25
12/16/2009		
9	18.9	0.24

Notes Added October 11, 2010

Calculations made with the DISNEL (68 F to 85 F) gave 0.016 %delta k per degree C

(The specifications on the reactor say 0.025% delta k per degree C.)

APPENDIX B – POWER CALIBRATION

Reactor Power Level as a Function of Channel No. 3 Detector Current

Reactor Power	Detector Current	Reactor Power	Detector Current	Reactor Power	Detector Current
10μW	6.94E-13	10mW	6.94E-10	2.0W	1.39E-07
20μW	1.39E-12	20mW	1.39E-09	2.1W	1.46E-07
30μW	2.08E-12	30mW	2.08E-09	2.2W	1.53E-07
40μW	2.78E-12	40mW	2.78E-09	2.3W	1.60E-07
50μW	3.47E-12	50mW	3.47E-09	2.4W	1.67E-07
60μW	4.16E-12	60mW	4.16E-09	2.5W	1.74E-07
70μW	4.86E-12	70mW	4.86E-09	2.6W	1.80E-07
80μW	5.55E-12	80mW	5.55E-09	2.7W	1.87E-07
90μW	6.25E-12	90mW	6.25E-09	2.8W	1.94E-07
				2.9W	2.01E-07
100μW	6.94E-12	100mW	6.94E-09	3.0W	2.08E-07
200μW	1.39E-11	200mW	1.39E-08	3.1W	2.15E-07
300μW	2.08E-11	300mW	2.08E-08	3.2W	2.22E-07
400μW	2.78E-11	400mW	2.78E-08	3.3W	2.29E-07
500μW	3.47E-11	500mW	3.47E-08	3.4W	2.36E-07
600μW	4.16E-11	600mW	4.16E-08	3.5W	2.43E-07
700μW	4.86E-11	700mW	4.86E-08	3.6W	2.50E-07
800μW	5.55E-11	800mW	5.55E-08	3.7W	2.57E-07
900μW	6.25E-11	900mW	6.25E-08	3.8W	2.64E-07
				3.9W	2.71E-07
1mW	6.94E-11	1.0W	6.94E-08	4.0W	2.78E-07
2mW	1.39E-10	1.1W	7.63E-08	4.1W	2.85E-07
3mW	2.08E-10	1.2W	8.33E-08	4.2W	2.91E-07
4mW	2.78E-10	1.3W	9.02E-08	4.3W	2.98E-07
5mW	3.47E-10	1.4W	9.72E-08	4.4W	3.05E-07
6mW	4.16E-10	1.5W	1.04E-07	4.5W	3.12E-07
7mW	4.86E-10	1.6W	1.11E-07	4.6W	3.19E-07
8mW	5.55E-10	1.7W	1.18E-07	4.7W	3.26E-07
9mW	6.25E-10	1.8W	1.25E-07	4.8W	3.33E-07
		1.9W	1.32E-07	4.9W	3.40E-07
				5.0W	3.47E-07

Approved 5/9/2012

 Reactor Supervisor

APPENDIX C – GOLD FOIL EXPERIMENT

Lab Manual for Gold Foil Experiment

Gold (197, 100%, a pure isotope) has a 98.7 barn thermal cross section.

However, it has a huge resonance at 4.9 eV.

Hence its resonance absorption will be very significant, whereas the resonance fission rate in the

AGN is very small.

The AGN-201 has 96.1% of the fission in the thermal range (below the cadmium cut off at 0.4

eV). Only 3.9% of the fissions occur above thermal. (2.3% in the resonance region, 0.4% in the

“fast” range, above 1 MeV, and the remainder between 0.4 eV and the resonance region).).

The Peak to average thermal flux in the core is 1.638.

1. Use the thermal (below 0.4 eV) activation of the gold = Bare counts - cadmium covered

counts to determine the peak thermal flux in the reactor, at the power level that the exposure was

made.

2. Then determine the fission rate at that location - i.e. fissions per second per cubic cm or per

gram of uranium -235, or some other reference value. Correct this fission rate to an average

fission rate for the entire core, and then using 672 grams of U-235, determine the total core

fission from thermal flux.

A) The total thermal flux can be obtained from the activation equation:

29

$$\text{Activity (dis/sec)} = \Sigma V \phi [1 - \exp(-\lambda t_e)][\exp(-\lambda t_d)]$$

where t_e = exposure time and t_d = decay time from end of exposure to the middle of count time.

B) Note that the $\Sigma V\phi$ term involves only the mass of the foil, not the volume, once you work out

the terms (i.e. the volume cancels out).

C) Solve the above for the thermal flux ϕ , and then determine the fission rate at that location.

D) If that is the peak flux location, then divide by 1.638, and divide by 0.961 to obtain the average total fission rate at that location (thermal plus epi-thermal). .

E) The total fission power will then be the average fission rate multiplied by the volume of the

core, since it is assumed that the core has uniform uranium density. (A minor correction can be

made for the “fuse.”)

F) Note that the exposure time (equivalent, steady state exposure) is a very critical parameter.

You would hope to know this value (equivalent) to about 1%.

(The decay time is also important, but its accuracy need not be smaller than a minute.)

Gold Foil Data

Foil	Mass	Position	Count
25	0.0139	-14	33824
8	0.0139	-13	36085
6	0.0139	-12	40871
10	0.014	-11	43622
18	0.0137	-10	47200
26	0.0137	-9	49874
4	0.0138	-8	53604
13	0.0139	-7	54397
12	0.0138	-6	57600
27	0.0142	-5	57413
21	0.0138	-4	60212
11	0.0138	-3	60534
19	0.0138	-2	59857
7	0.0137	-1	59569
5	0.0139	0	59695
1	0.0136	1	59405
29	0.0136	2	61442
2	0.0137	3	61664
14	0.0136	4	57928
3	0.0139	5	58723
9	0.0138	6	57134
15	0.0135	7	53264
16	0.0139	8	53144
23	0.0139	9	50292
20	0.0141	10	46127
24	0.0139	11	43003
28	0.014	12	38943
22	0.0141	13	36050
17	0.0138	14	32861

APPENDIX D – MATLAB CODES

“Cylinder” MATLAB Code

```
clear
% Find all windows of type figure, which have an empty FileName
attribute.
allPlots = findall(0, 'Type', 'figure', 'FileName', []);
delete(allPlots);

%Flux data
Flux = [57354, 56444, 57169, 57852, 57583, 56532, 55157, 52501,
51395, 47503, 44984, 42509, 39567, 34958];%, 32788];

r_mes = [0, 1, 2, 3, 4, 5, 6, 7, 8, 9, 10, 11, 12, 13]; %, 14];

Fluxtimesr = Flux.*r_mes;
%Constants
R = 12.8; %Core Radius
Z = 12.35; %Half Core Height
Lambda = 2.405/R;
D = pi/(2*Z);
P = 4.9; %Power level in watts
V = pi*R^2*Z;
k = 0.00599;%0.003349; %Thermal conductivity w/cmK
%A_TEMP = P*Lambda/(4*Z*R*k*BESSELJ(1,Lambda*R))
A = P/(4*Z*k*trapz(Fluxtimesr))
Cp = 1.801;%2.302; %Specific heat J/gK
rho = 1.234;%0.96%1.2474; %density g/cm^3      0.92 used previously
alpha = 60*k/(Cp*rho) %cm^2/min

Time = 2000; %Total time in minutes

%Incraments
delta_r = 0.2;
delta_z = 0.2;
delta_t = 1;
tol = 0.001

Rmax = ceil(R/delta_r);
Zmax = ceil(Z/delta_z);
Tmax = ceil(Time/delta_t);

%r = 0:Rmax;
%z = 0:Zmax;

points = (Rmax + 1)*(Zmax + 1);

%Create coefficient matrix, variable vector, and constants vector
coefs = zeros(points, points);
```

```

vars = zeros(points, Tmax+1);
consts = zeros(points, 1);

coefs_ss = zeros(points, points);
vars_ss = zeros(points, 1);
consts_ss = zeros(points, 1);

oneoverrrsq = 1/delta_r^2;
oneoverzsq = 1/delta_z^2;
alphadt = 1/(alpha*delta_t);

start_time = clock;

for z_int = 0:Zmax
    for r_int = 0:Rmax
        index = z_int*Rmax+r_int+z_int+1;
        r = r_int*delta_r;
        z = z_int*delta_z;
        switch true
            case(r == 0 & z == 0)
                coefs_ss(index,index) = -2*oneoverrrsq -2*oneoverzsq;
                coefs_ss(index,index+1) = 2*oneoverrrsq;
                coefs_ss(index,index+1+Rmax) = 2*oneoverzsq;
                %consts(index) = -A*BESSELJ(0,Lambda*r)*cos(D*z);
                consts_ss(index) = -
A*interp1(r_mes,Flux,r)*cos(D*z);
            case(r == 0 & z > 0 & z < Z)
                coefs_ss(index,index) = -2*oneoverrrsq -2*oneoverzsq;
                coefs_ss(index,index+1) = 2*oneoverrrsq;
                coefs_ss(index,index+1+Rmax) = oneoverzsq;
                coefs_ss(index,index-1-Rmax) = oneoverrrsq;
                %consts(index) = -A*BESSELJ(0,Lambda*r)*cos(D*z);
                consts_ss(index) = -
A*interp1(r_mes,Flux,r)*cos(D*z);
            case(r > 0 & r < R & z == 0)
                coefs_ss(index,index) = -2*oneoverrrsq -2*oneoverzsq;
                coefs_ss(index,index+1) = oneoverrrsq +
1/(r*2*delta_r);
                coefs_ss(index,index-1) = oneoverrrsq -
1/(r*2*delta_r);
                coefs_ss(index,index+1+Rmax) = 2*oneoverzsq;
                %consts(index) = -A*BESSELJ(0,Lambda*r)*cos(D*z);
                consts_ss(index) = -
A*interp1(r_mes,Flux,r)*cos(D*z);
            case(r >= R | z >= Z)
                coefs_ss(index,index) = 1;
                consts_ss(index) = 0;
            otherwise
                coefs_ss(index,index) = -2*oneoverrrsq -2*oneoverzsq;
                coefs_ss(index,index+1) = oneoverrrsq +
1/(r*2*delta_r);
                coefs_ss(index,index-1) = oneoverrrsq -
1/(r*2*delta_r);

```

```

        coefs_ss(index,index+1+Rmax) = oneoverzsq;
        coefs_ss(index,index-1-Rmax) = oneoverrrsq;
        %consts(index) = -A*BESSELJ(0,Lambda*r)*cos(D*z);
        consts_ss(index) = -
A*interp1(r_mes,Flux,r)*cos(D*z);
    end
end
end

vars_ss = inv(coefs_ss)*consts_ss;

for t = 2:Tmax+1

for z_int = 0:Zmax
    for r_int = 0:Rmax
        index = z_int*Rmax+r_int+z_int+1;
        r = r_int*delta_r;
        z = z_int*delta_z;
        switch true
            case(r == 0 & z == 0)
                coefs(index,index) = -2*oneoverrrsq -2*oneoverzsq -
alphadt;
                coefs(index,index+1) = 2*oneoverrrsq;
                coefs(index,index+1+Rmax) = 2*oneoverzsq;
                %consts(index) = -A*BESSELJ(0,Lambda*r)*cos(D*z);
                consts(index) = -A*interp1(r_mes,Flux,r)*cos(D*z) -
alphadt*vars(index,t-1);
            case(r == 0 & z > 0 & z < Z)
                coefs(index,index) = -2*oneoverrrsq -2*oneoverzsq -
alphadt;
                coefs(index,index+1) = 2*oneoverrrsq;
                coefs(index,index+1+Rmax) = oneoverzsq;
                coefs(index,index-1-Rmax) = oneoverrrsq;
                %consts(index) = -A*BESSELJ(0,Lambda*r)*cos(D*z);
                consts(index) = -A*interp1(r_mes,Flux,r)*cos(D*z) -
alphadt*vars(index,t-1);
            case(r > 0 & r < R & z == 0)
                coefs(index,index) = -2*oneoverrrsq -2*oneoverzsq -
alphadt;
                coefs(index,index+1) = oneoverrrsq + 1/(r*2*delta_r);
                coefs(index,index-1) = oneoverrrsq - 1/(r*2*delta_r);
                coefs(index,index+1+Rmax) = 2*oneoverzsq;
                %consts(index) = -A*BESSELJ(0,Lambda*r)*cos(D*z);
                consts(index) = -A*interp1(r_mes,Flux,r)*cos(D*z) -
alphadt*vars(index,t-1);
            case(r >= R | z >= Z)
                coefs(index,index) = 1;
                consts(index) = 0;
            otherwise
                coefs(index,index) = -2*oneoverrrsq -2*oneoverzsq -
alphadt;
                coefs(index,index+1) = oneoverrrsq + 1/(r*2*delta_r);
                coefs(index,index-1) = oneoverrrsq - 1/(r*2*delta_r);
                coefs(index,index+1+Rmax) = oneoverzsq;

```



```

        coefs(index,index-1-Rmax) = oneoverrsq;
        %consts(index) = -A*BESSELJ(0,Lambda*r)*cos(D*z);
        consts(index) = -A*interp1(r_mes,Flux,r)*cos(D*z) -
alphadt*vars(index,t-1);
        end
    end
end
vars(:,t) = inv(coefs)*consts;
disp(t-1)

r_temp = 0:Rmax;
r = r_temp * delta_r;
%vars(1:Rmax+1,t);      I don't remember what this is doing

plot(r, vars(1:Rmax+1,t));
axis([0,14,0,8])
xlabel('Radial Distance (cm)')
ylabel('Change in Temp (C) at Z = 0')
drawnow

if (abs(vars(:,t)-vars_ss) < max(vars_ss.*tol))
    disp('steady state reached at')
    t_ss = t - 1
    disp('Time constant is:')
    timeconst = -log(tol)/t_ss %log in Matlab is ln
    break;

end
end

end_time = clock;

t_temp = 0:Tmax;
times = t_temp * delta_t;

figure
plot(times, vars(1,:))
xlabel('Time (min)')
ylabel('Change in Temp at the Orgin (C)')

save('Cylinder2new')

```

“Sphere” MATLAB Code

```
clear
% Find all windows of type figure, which have an empty FileName
attribute.
allPlots = findall(0, 'Type', 'figure', 'FileName', []);
delete(allPlots);

%Flux data
Flux = [57354, 56444, 57169, 57852, 57583, 56532, 55157, 52501,
51395, 47503, 44984, 42509, 39567, 34958, 32788];

r_mes = [0, 1, 2, 3, 4, 5, 6, 7, 8, 9, 10, 11, 12, 13, 14];

Fluxtimesr = Flux.*r_mes.*r_mes;
%Constants
R = 14.48; %Core Radius
Z = 11.9; %Half Core Height
Lambda = 2.405/(1.2*R);
D = pi/(2.2*Z);
P = 4.9; %Power level in watts
V = 4/3*pi*R^3;
k = 0.00599; %0.003349; %Thermal conductivity w/cmK
%A = P*Lambda/(4*2*Z*R*k*BESSELJ(1,Lambda*R));
%R_s = (0.75*R^2*2*Z)^(1/3)
A = P/(4*pi*k*trapz(Fluxtimesr));
Cp = 1.801;%2.302; %Specific heat J/gK
rho = 1.234; %0.96; %density g/cm^3
alpha = 60*k/(Cp*rho) %cm^2/min

Time = 2000; %Total time in minutes
tol = 0.001

%Incraments
delta_r = .01;
delta_t = 1;

Rmax = ceil(R/delta_r);
Tmax = ceil(Time/delta_t);

%r = 0:Rmax;
%z = 0:Zmax;

points = (Rmax + 1)

%Create coefficent matrix, variable vector, and constants vector

coefs = zeros(points, points);
vars = zeros(points, Tmax+1);
consts = zeros(points, 1);
```

```

coefs_ss = zeros(points, points);
vars_ss = zeros(points, 1);
consts_ss = zeros(points, 1);

oneoverrrsq = 1/delta_r^2;
alphadt = 1/(alpha*delta_t);

start_time = clock;

for r_int = 0:Rmax
    index = r_int + 1; %index can't be 0
    r = r_int*delta_r;

    switch true
        case(r == 0)
            coefs_ss(index,index) = -2*oneoverrrsq;
            coefs_ss(index,index+1) = 2*oneoverrrsq;
            consts_ss(index) = -
A*interp1(r_mes,Flux,r,'spline','extrap');
        case(r >= R)
            coefs_ss(index,index) = 1;
            consts_ss(index) = 0;
        otherwise
            coefs_ss(index,index) = -2*oneoverrrsq;
            coefs_ss(index,index+1) = oneoverrrsq +
1/(r*delta_r);
            coefs_ss(index,index-1) = oneoverrrsq -
1/(r*delta_r);
            consts_ss(index) = -
A*interp1(r_mes,Flux,r,'spline','extrap');
    end
end
vars_ss = inv(coefs_ss)*consts_ss;

for t = 2:Tmax+1

    for r_int = 0:Rmax
        index = r_int + 1; %index can't be 0
        r = r_int*delta_r;

        switch true
            case(r == 0)
                coefs(index,index) = -2*oneoverrrsq -alphadt;
                coefs(index,index+1) = 2*oneoverrrsq;
                consts(index) = -
A*interp1(r_mes,Flux,r,'spline','extrap') -alphadt*vars(index,t-1);
            case(r >= R)
                coefs(index,index) = 1;
                consts(index) = 0;
            otherwise
                coefs(index,index) = -2*oneoverrrsq -alphadt;

```

```

        coefs(index,index+1) = oneoverrsq + 1/(r*delta_r);
        coefs(index,index-1) = oneoverrsq - 1/(r*delta_r);
        consts(index) = -
A*interp1(r_mes,Flux,r,'spline','extrap') -alphadt*vars(index,t-1);
    end
    end
vars(:,t) = inv(coefs)*consts;
disp(t-1)

r_temp = 0:Rmax;
r = r_temp * delta_r;
%vars(1:Rmax+1,t);      I don't remember what this is doing

plot(r, vars(1:Rmax+1,t));
axis([0,14,0,8])
xlabel('Radial Distance (cm)')
ylabel('Change in Temp (C)')
drawnow

if (abs(vars(:,t)-vars_ss) < max(vars_ss.*tol))
    disp('steady state reached at')
    t_ss = (t - 1) * delta_t
    disp('Time constant is:')
    timeconst = -log(tol)/t_ss %log in Matlab is ln
    break;

end

end

end_time = clock;

t_temp = 0:Tmax;
times = t_temp * delta_t;

figure
plot(times, vars(1,:))
xlabel('Time (min)')
ylabel('Change in Temp at the Orgin (C)')

avg_temp = 4*pi*trapz(vars(:,t)'.*r.*r)/V*delta_r %delta_r
comensates for trapz unit spacing
joules = rho*V*Cp*avg_temp
wattminutes = joules/60

Q_dot = (vars(Rmax+1,t)-vars(Rmax,t))/delta_r*k*4*pi*R^2

save('14cmSphere01')

```

“AverageTemps” MATLAB Code

```
clear
% Find all windows of type figure, which have an empty FileName
attribute.
allPlots = findall(0, 'Type', 'figure', 'FileName', []);
delete(allPlots);

load('14cmSphere01')
Rfuse = 0.5;

timestep = 200;
numtimes = ceil(t_ss*delta_t/timestep)+1;
times = 0:timestep:t_ss;

if(length(times) ~= numtimes)
    times(numtimes) = t_ss;
end

times

for(j=1:numtimes)
    timesindex(j) = ceil(times(j)/delta_t)+1;
end

%{
R
Z
Lambda = 2.405/(1.2*R);
D = pi/(2.2*Z);
P = 4.9; %Power level in watts
V = 4/3*pi*R^3;
k = 0.00599; %0.003349; %Thermal conductivity w/cmK
%A = P*Lambda/(4*2*Z*R*k*BESSELJ(1,Lambda*R));
%R_s = (0.75*R^2*2*Z)^(1/3)
A = P/(4*pi*k*trapz(Fluxtimesr));
Cp = 1.801;%2.302; %Specific heat J/gK
rho = 1.234; %0.96; %density g/cm^3
alpha = 60*k/(Cp*rho) %cm^2/min

Time = 2000; %Total time in minutes
tol = 0.001

%Incraments
delta_r = .01;
delta_t = 1;

Rmax = ceil(R/delta_r);
Tmax = ceil(Time/delta_t);

%r = 0:Rmax;
%z = 0:Zmax;
```

```

points = (Rmax + 1)

%Create coefficient matrix, variable vector, and constants vector

%coefs = zeros(points, points);
%vars = zeros(points, Tmax+1);
%consts = zeros(points, 1);


t_temp = 0:Tmax;
times = t_temp * delta_t;

figure
plot(times, vars(1,:))
xlabel('Time (min)')
ylabel('Change in Temp at the Orgin (C)')

avg_temp = 4*pi*trapz(vars(:,t)).*r.*r)/V*delta_r %delta_r
comensates for trapz unit spacing
joules = rho*V*Cp*avg_temp
wattminutes = joules/60

Q_dot = (vars(Rmax+1,t)-vars(Rmax,t))/delta_r*k*4*pi*R^2

%}

regions = 3;

avetemps = zeros(numtimes, regions);
Rinners = zeros(regions, 2); %Fist is the value 2nd is the indicy in
r
Routers = zeros(regions, 2);

if(regions == 1)
    Rinners(1,1) = 0;
    Rinners(1,2) = 1;
    Routters = r(length(r));
    Routters = length(r);
else
    %First region is always going to be the thermal fuse in a
multiregion
    %problem
    Rinners(1,1) = 0;
    Rinners(1,2) = 1;
    Routters(1,2) = ceil(Rfuse/delta_r)+1;
    Routters(1,1) = r(Routers(1,2));

```

```

LORegions = (R-Rfuse)/(regions-1); %Length of outter regions

i = 2;
while(i <= regions)
    Ridders(i,1) = Routters(i-1,1);
    Ridders(i,2) = Routters(i-1,2);
    Routters(i,2) = ceil((LORegions*(i-1) + Rfuse)/delta_r)+1;
    Routters(i,1) = r(Routers(i,2));

    i = i + 1;
end

end

for(j = 1:numtimes)
    for(k = 1:regions)
        regiontemps =
vars(Ridders(k,2):Routers(k,2),timesindex(j));
        regionRs = r(Ridders(k,2):Routers(k,2));
        avetemps(j,k) =
3*trapz(regionRs,regiontemps.*regionRs'.*regionRs')/(Routers(k,1)^3
- Ridders(k,1)^3);
    end
    times(j)
    Ridders(:,1)'
    Routters(:,1)'
    avetemps(j,:)
end

```

APPENDIX E – DISNEL CODES

“1 region sphere 68F” DISNEL Code

```

0
19 1      AGN 201 equivalent sphere, 14.48 cm radius/fuse
      5      1      1
      1      2      3      3      68.00
      1      950.00026806
      1      98      0.001072      12
      0.89      0.46      0.50      1.00      1.0      1.0
1.0      1.0
      0      6      0.040189
      0      1      0.080378
      0      8      0.0013378
      2      2      3      3      68.00
      1      950.00013403
      1      98      0.000536      12
      0.70      0.46      0.50      1.00      1.0      1.0
1.0      1.0
      0      6      0.040189
      0      1      0.080378
      0      8      0.0013378
      3      2      3      3      68.00
      1      95      0.000135
      1      98      0.000791      12
      0.70      0.46      0.50      1.0      1.0      1.0
1.0      1.0
      0      6      0.0396
      0      1      0.0791
      0      13      0.00052
      4      0      1      3      68.00
      0      6      0.0878
      5      0      1      3      68.00
      0      79      0.00591
      4      0      3      4      4      2      4      1      1      20      1      1      0
100
      0.0      0.0      0.0000      .00000001      0.0001      0
      1      5      0.5      0.0000      2      80      13.98      0.00000
      4      100      20.0      0.00000

```


“1 region sphere 108F SS” DISNEL Code

```

0
19 1    AGN 201 equivalent sphere, 14.48 cm radius/fuse
      5      1      1
      1      2      3      3      108.00
      1      950.00026787
      1      980.00107123 12
      0.89      0.47      0.51      1.00      1.0      1.0
1.0      1.0
      0      60.04016006
      0      10.08032013
      0      80.00133684
      2      2      3      3      108.00
      1      950.00013393
      1      980.00053561 12
      0.70      0.47      0.51      1.00      1.0      1.0
1.0      1.0
      0      60.04016006
      0      10.08032013
      0      80.00133684
      3      2      3      3      68.00
      1      95  0.000135
      1      98  0.000791 12
      0.70      0.46      0.50      1.0      1.0      1.0
1.0      1.0
      0      6      0.0396
      0      1      0.0791
      0      13      0.00052
      4      0      1      3      68.00
      0      6      0.0878
      5      0      1      3      68.00
      0      79      0.00591
      4      0      3      4      4      2      4      1      1      20      1      1      0
100
      0.0      0.0      0.0000      .00000001      0.0001      0
      1      50.50012000      0.0000      2      8013.9833552      0.00000
      4      100      20.0      0.00000

```

“1 region sphere 100W” DISNEL Code

```

0
19 1    AGN 201 equivalent sphere, 14.48 cm radius/fuse
      5    1    1
      1    2    3    3 98.884220
      1    950.00026791
      1    980.00107140 12
      0.89    0.46    0.50    1.00    1.0    1.0
1.0      1.0
      0    60.04016666
      0    10.08033332
      0    80.00133706
      2    2    3    3 98.884220
      1    950.00013396
      1    980.00053570 12
      0.70    0.46    0.50    1.00    1.0    1.0
1.0      1.0
      0    60.04016666
      0    10.08033332
      0    80.00133706
      3    2    3    3    68.00
      1    95    0.000135
      1    98    0.000791 12
      0.70    0.46    0.50    1.0    1.0    1.0
1.0      1.0
      0    6    0.0396
      0    1    0.0791
      0    13    0.00052
      4    0    1    3    68.00
      0    6    0.0878
      5    0    1    3    68.00
      0    79    0.00591
      4    0    3    4    4    2    4    1    1    20    1    1    0
100
      0.0    0.0    0.0000    .00000001    0.0001    0
      1    50.50009265    0.0000    2    8013.9825905    0.00000
      4    100    20.0    0.00000

```

“1 region sphere t100” DISNEL Code

```

0
19 1    AGN 201 equivalent sphere, 14.48 cm radius/fuse
      5    1    1
      1    2    3    3 68.941940
      1    950.00026806
      1    980.00107198 12
      0.89    0.46    0.50    1.00    1.0    1.0
1.0      1.0
      0    60.04018832
      0    10.08037664
      0    80.00133778
      2    2    3    3 68.941940
      1    950.00013403
      1    980.00053599 12
      0.70    0.46    0.50    1.00    1.0    1.0
1.0      1.0
      0    60.04018832
      0    10.08037664
      0    80.00133778
      3    2    3    3    68.00
      1    95    0.000135
      1    98    0.000791 12
      0.70    0.46    0.50    1.0    1.0    1.0
1.0      1.0
      0    6    0.0396
      0    1    0.0791
      0    13    0.00052
      4    0    1    3    68.00
      0    6    0.0878
      5    0    1    3    68.00
      0    79    0.00591
      4    0    3    4    4    2    4    1    1    20    1    1    0
100
      0.0    0.0    0.0000    .00000001    0.0001    0
      1    50.50000283    0.0000    2    8013.9800790    0.00000
      4    100    20.0    0.00000

```

“1 region sphere t200” DISNEL Code

```

0
19 1    AGN 201 equivalent sphere, 14.48 cm radius/fuse
      5    1    1
      1    2    3    3 69.282860
      1    950.00026805
      1    980.00107198 12
      0.89    0.46    0.50    1.00    1.0    1.0
1.0      1.0
      0    60.04018807
      0    10.08037614
      0    80.00133777
      2    2    3    3 69.282860
      1    950.00013403
      1    980.00053599 12
      0.70    0.46    0.50    1.00    1.0    1.0
1.0      1.0
      0    60.04018807
      0    10.08037614
      0    80.00133777
      3    2    3    3    68.00
      1    95    0.000135
      1    98    0.000791 12
      0.70    0.46    0.50    1.0    1.0    1.0
1.0      1.0
      0    6    0.0396
      0    1    0.0791
      0    13    0.00052
      4    0    1    3    68.00
      0    6    0.0878
      5    0    1    3    68.00
      0    79    0.00591
      4    0    3    4    4    2    4    1    1    20    1    1    0
100
      0.0    0.0    0.0000    .00000001    0.0001    0
      1    50.50000385    0.0000    2    8013.9801076    0.00000
      4    100    20.0    0.00000

```

“1 region sphere t300” DISNEL Code

```

0
19 1    AGN 201 equivalent sphere, 14.48 cm radius/fuse
      5    1    1
      1    2    3    3 69.416600
      1    950.00026805
      1    980.00107197 12
      0.89    0.46    0.50    1.00    1.0    1.0
1.0      1.0
      0    60.04018798
      0    10.08037595
      0    80.00133777
      2    2    3    3 69.416600
      1    950.00013403
      1    980.00053599 12
      0.70    0.46    0.50    1.00    1.0    1.0
1.0      1.0
      0    60.04018798
      0    10.08037595
      0    80.00133777
      3    2    3    3    68.00
      1    95    0.000135
      1    98    0.000791 12
      0.70    0.46    0.50    1.0    1.0    1.0
1.0      1.0
      0    6    0.0396
      0    1    0.0791
      0    13    0.00052
      4    0    1    3    68.00
      0    6    0.0878
      5    0    1    3    68.00
      0    79    0.00591
      4    0    3    4    4    2    4    1    1    20    1    1    0
100
      0.0    0.0    0.0000    .00000001    0.0001    0
      1    50.50000425    0.0000    2    8013.9801188    0.00000
      4    100    20.0    0.00000

```

“1 region sphere t400” DISNEL Code

```

0
19 1    AGN 201 equivalent sphere, 14.48 cm radius/fuse
      5    1    1
      1    2    3    3 69.469160
      1    950.00026805
      1    980.00107197 12
      0.89    0.46    0.50    1.00    1.0    1.0
1.0      1.0
      0    60.04018794
      0    10.08037587
      0    80.00133776
      2    2    3    3 69.469160
      1    950.00013403
      1    980.00053599 12
      0.70    0.46    0.50    1.00    1.0    1.0
1.0      1.0
      0    60.04018794
      0    10.08037587
      0    80.00133776
      3    2    3    3    68.00
      1    95    0.000135
      1    98    0.000791 12
      0.70    0.46    0.50    1.0    1.0    1.0
1.0      1.0
      0    6    0.0396
      0    1    0.0791
      0    13    0.00052
      4    0    1    3    68.00
      0    6    0.0878
      5    0    1    3    68.00
      0    79    0.00591
      4    0    3    4    4    2    4    1    1    20    1    1    0
100
      0.0    0.0    0.0000    .00000001    0.0001    0
      1    50.50000441    0.0000    2    8013.9801232    0.00000
      4    100    20.0    0.00000

```

“1 region sphere t500” DISNEL Code

```

0
19 1    AGN 201 equivalent sphere, 14.48 cm radius/fuse
      5    1    1
      1    2    3    3 69.490040
      1    950.00026805
      1    980.00107197 12
      0.89    0.46    0.50    1.00    1.0    1.0
1.0      1.0
      0    60.04018792
      0    10.08037584
      0    80.00133776
      2    2    3    3 69.490040
      1    950.00013403
      1    980.00053599 12
      0.70    0.46    0.50    1.00    1.0    1.0
1.0      1.0
      0    60.04018792
      0    10.08037584
      0    80.00133776
      3    2    3    3    68.00
      1    95    0.000135
      1    98    0.000791 12
      0.70    0.46    0.50    1.0    1.0    1.0
1.0      1.0
      0    6    0.0396
      0    1    0.0791
      0    13    0.00052
      4    0    1    3    68.00
      0    6    0.0878
      5    0    1    3    68.00
      0    79    0.00591
      4    0    3    4    4    2    4    1    1    20    1    1    0
100
      0.0    0.0    0.0000    .00000001    0.0001    0
      1    50.50000447    0.0000    2    8013.9801250    0.00000
      4    100    20.0    0.00000

```

“1 region sphere t600” DISNEL Code

```

0
19 1    AGN 201 equivalent sphere, 14.48 cm radius/fuse
      5    1    1
      1    2    3    3 69.498140
      1    950.00026805
      1    980.00107197 12
      0.89    0.46    0.50    1.00    1.0    1.0
1.0      1.0
      0    60.04018794
      0    10.08037587
      0    80.00133776
      2    2    3    3 69.498140
      1    950.00013403
      1    980.00053599 12
      0.70    0.46    0.50    1.00    1.0    1.0
1.0      1.0
      0    60.04018794
      0    10.08037587
      0    80.00133776
      3    2    3    3    68.00
      1    95    0.000135
      1    98    0.000791 12
      0.70    0.46    0.50    1.0    1.0    1.0
1.0      1.0
      0    6    0.0396
      0    1    0.0791
      0    13    0.00052
      4    0    1    3    68.00
      0    6    0.0878
      5    0    1    3    68.00
      0    79    0.00591
      4    0    3    4    4    2    4    1    1    20    1    1    0
100      0.0    0.0    0.0000    .00000001    0.0001    0
      1    50.50000449    0.0000    2    8013.9801257    0.00000
      4    100    20.0    0.00000

```


“1 region sphere t700” DISNEL Code

```

0
19 1    AGN 201 equivalent sphere, 14.48 cm radius/fuse
      5    1    1
      1    2    3    3 69.501380
      1    950.00026805
      1    980.00107197 12
      0.89    0.46    0.50    1.00    1.0    1.0
1.0      1.0
      0    60.04018794
      0    10.08037587
      0    80.00133776
      2    2    3    3 69.501380
      1    950.00013403
      1    980.00053599 12
      0.70    0.46    0.50    1.00    1.0    1.0
1.0      1.0
      0    60.04018794
      0    10.08037587
      0    80.00133776
      3    2    3    3    68.00
      1    95    0.000135
      1    98    0.000791 12
      0.70    0.46    0.50    1.0    1.0    1.0
1.0      1.0
      0    6    0.0396
      0    1    0.0791
      0    13    0.00052
      4    0    1    3    68.00
      0    6    0.0878
      5    0    1    3    68.00
      0    79    0.00591
      4    0    3    4    4    2    4    1    1    20    1    1    0
100
      0.0    0.0    0.0000    .00000001    0.0001    0
      1    50.50000450    0.0000    2    8013.9801259    0.00000
      4    100    20.0    0.00000

```

“1 region sphere t757” DISNEL Code

```

0
19 1    AGN 201 equivalent sphere, 14.48 cm radius/fuse
      5    1    1
      1    2    3    3 69.502280
      1    950.00026805
      1    980.00107197 12
      0.89    0.46    0.50    1.00    1.0    1.0
1.0      1.0
      0    60.04018794
      0    10.08037587
      0    80.00133776
      2    2    3    3 69.502280
      1    950.00013403
      1    980.00053599 12
      0.70    0.46    0.50    1.00    1.0    1.0
1.0      1.0
      0    60.04018794
      0    10.08037587
      0    80.00133776
      3    2    3    3    68.00
      1    95    0.000135
      1    98    0.000791 12
      0.70    0.46    0.50    1.0    1.0    1.0
1.0      1.0
      0    6    0.0396
      0    1    0.0791
      0    13    0.00052
      4    0    1    3    68.00
      0    6    0.0878
      5    0    1    3    68.00
      0    79    0.00591
      4    0    3    4    4    2    4    1    1    20    1    1    0
100
      0.0    0.0    0.0000    .00000001    0.0001    0
      1    50.50000451    0.0000    2    8013.9801260    0.00000
      4    100    20.0    0.00000

```

"2 region sphere 68F" DISNEL Code

```

0
19 1    AGN 201 equivalent sphere, 14.48 cm radius/fuse
      5    1    1
      1    2    3    3    68.00
      1    950.00026806
      1    98    0.001072    12
          0.89    0.46    0.50    1.00    1.0    1.0
1.0      1.0
      0    6    0.040189
      0    1    0.080378
      0    8    0.0013378
      2    2    3    3    68.00
      1    950.00013403
      1    98    0.000536    12
          0.70    0.46    0.50    1.00    1.0    1.0
1.0      1.0
      0    6    0.040189
      0    1    0.080378
      0    8    0.0013378
      3    2    3    3    68.00
      1    95    0.000135
      1    98    0.000791    12
          0.70    0.46    0.50    1.0    1.0    1.0
1.0      1.0
      0    6    0.0396
      0    1    0.0791
      0    13    0.00052
      4    0    1    3    68.00
      0    6    0.0878
      5    0    1    3    68.00
      0    79    0.00591
      4    0    3    4    4    2    4    1    1    20    1    1    0
100
      0.0    0.0    0.0000    .00000001    0.0001    0
      1    5    0.5    0.0000    2    80    13.98    0.00000
      4    100    20.0    0.00000

```

“2 region sphere t400” DISNEL Code

```

0
19 1    AGN 201 equivalent sphere, 14.48 cm radius/fuse
      5    1    1
      1    2    3    3 71.941640
      1    950.00026804
      1    980.00107192 12
      0.89    0.46    0.50    1.00    1.0    1.0
1.0      1.0
      0    60.04018615
      0    10.08037230
      0    80.00133771
      2    2    3    3 69.469160
      1    950.00013403
      1    980.00053599 12
      0.70    0.46    0.50    1.00    1.0    1.0
1.0      1.0
      0    60.04018794
      0    10.08037587
      0    80.00133776
      3    2    3    3    68.00
      1    95    0.000135
      1    98    0.000791 12
      0.70    0.46    0.50    1.0    1.0    1.0
1.0      1.0
      0    6    0.0396
      0    1    0.0791
      0    13    0.00052
      4    0    1    3    68.00
      0    6    0.0878
      5    0    1    3    68.00
      0    79    0.00591
      4    0    3    4    4    2    4    1    1    20    1    1    0
100
      0.0    0.0    0.0000    .00000001    0.0001    0
      1    50.50001182    0.0000    2    8013.9801232    0.00000
      4    100    20.0    0.00000

```

"3 region sphere 68F" DISNEL Code

```

0
19 1    AGN 201 equivalent sphere, 14.48 cm radius/fuse
      5    1    1
      1    2    3    3    68.00
      1    950.00026806
      1    98    0.001072    12
      0.89    0.46    0.50    1.00    1.0    1.0
1.0      1.0
      0    6    0.040189
      0    1    0.080378
      0    8    0.0013378
      2    2    3    3    68.00
      1    950.00013403
      1    98    0.000536    12
      0.70    0.46    0.50    1.00    1.0    1.0
1.0      1.0
      0    6    0.040189
      0    1    0.080378
      0    8    0.0013378
      3    2    3    3    68.00
      1    950.00013403
      1    98    0.000536    12
      0.70    0.46    0.50    1.00    1.0    1.0
1.0      1.0
      0    6    0.040189
      0    1    0.080378
      0    8    0.0013378
      4    0    1    3    68.00
      0    6    0.0878
      5    0    1    3    68.00
      0    79    0.00591
      4    0    4    4    4    2    4    1    1    20    1    1    0
100
      0.0    0.0    0.0000    .00000001    0.0001    0
      1    5    0.5    0.0000    2    40    6.99    0.00000
      3    40    6.99    0.0000    4    100    20.0    0.00000

```

“3 region sphere t400” DISNEL Code

```

0
19 1    AGN 201 equivalent sphere, 14.48 cm radius/fuse
      5      1      1
      1      2      3      3 71.941640
      1      950.00026804
      1      980.00107192 12
      0.89      0.46      0.50      1.00      1.0      1.0
1.0      1.0
      0      60.04018615
      0      10.08037230
      0      80.00133771
      2      2      3      3 71.236220
      1      950.00013402
      1      980.00053597 12
      0.70      0.46      0.50      1.00      1.0      1.0
1.0      1.0
      0      60.04018666
      0      10.08037332
      0      80.00133772
      3      2      3      3 69.185300
      1      950.00013403
      1      980.00053599 12
      0.70      0.46      0.50      1.00      1.0      1.0
1.0      1.0
      0      60.04018814
      0      10.08037629
      0      80.00133777
      4      0      1      3      68.00
      0      6      0.0878
      5      0      1      3      68.00
      0      79      0.00591
      4      0      4      4      4      2      4      1      1      20      1      1      0
100
      0.0      0.0      0.0000      .00000001      0.0001      0
      1      50.50001182      0.0000      2      406.99013573      0.00000
      3      406.99004971      0.0000      4      100      20.0      0.00000

```

“4 region sphere 68F” DISNEL Code

```

0
19 1    AGN 201 equivalent sphere, 14.48 cm radius/fuse
      5      1      1
      1      2      3      3      68.00
      1      950.00026806
      1      98      0.001072      12
      0.89      0.46      0.50      1.00      1.0      1.0
1.0      1.0
      0      6      0.040189
      0      1      0.080378
      0      8      0.0013378
      2      2      3      3      68.00
      1      950.00013403
      1      98      0.000536      12
      0.70      0.46      0.50      1.00      1.0      1.0
1.0      1.0
      0      6      0.040189
      0      1      0.080378
      0      8      0.0013378
      3      2      3      3      68.00
      1      950.00013403
      1      98      0.000536      12
      0.70      0.46      0.50      1.00      1.0      1.0
1.0      1.0
      0      6      0.040189
      0      1      0.080378
      0      8      0.0013378
      4      2      3      3      68.00
      1      950.00013403
      1      98      0.000536      12
      0.70      0.46      0.50      1.00      1.0      1.0
1.0      1.0
      0      6      0.040189
      0      1      0.080378
      0      8      0.0013378
      5      0      1      3      68.00
      0      6      0.0878
      4      0      5      4      4      2      4      1      1      20      1      1      0
100
      0.0      0.0      0.0000      .00000001      0.0001      0
      1      5      0.5      0.0000      2      27      4.66      0.00000
      3      27      4.66      0.0000      4      27      4.66      0.00000
      5      100      20.0      0.00000

```

“4 region sphere t400” DISNEL Code

```

0
19 1    AGN 201 equivalent sphere, 14.48 cm radius/fuse
      5      1      1
      1      2      3      3 71.941640
      1      950.00026804
      1      980.00107192 12
      0.89      0.46      0.50      1.00      1.0      1.0
1.0      1.0
      0      60.04018615
      0      10.08037230
      0      80.00133771
      2      2      3      3 71.607740
      1      950.00013402
      1      980.00053597 12
      0.70      0.46      0.50      1.00      1.0      1.0
1.0      1.0
      0      60.04018639
      0      10.08037278
      0      80.00133771
      3      2      3      3 70.595960
      1      950.00013402
      1      980.00053597 12
      0.70      0.46      0.50      1.00      1.0      1.0
1.0      1.0
      0      60.04018712
      0      10.08037424
      0      80.00133774
      4      2      3      3 68.891900
      1      950.00013403
      1      980.00053599 12
      0.70      0.46      0.50      1.00      1.0      1.0
1.0      1.0
      0      60.04018835
      0      10.08037671
      0      80.00133778
      5      0      1      3      68.00
      0      6      0.0878
      4      0      5      4      4      2      4      1      1      20      1      1      0
100
      0.0      0.0      0.0000      .0000001      0.0001      0
      1      50.50001182      0.0000      2      274.66010087      0.00000
      3      274.66007258      0.0000      4      274.66002494      0.00000
      5      100      20.0      0.00000

```


“5 region sphere 68F” DISNEL Code

```

0
19 1    AGN 201 equivalent sphere, 14.48 cm radius/fuse
      6      1      1
      1      2      3      3      68.00
      1      950.00026806
      1      98      0.001072      12
      0.89      0.46      0.50      1.00      1.0      1.0
1.0      1.0
      0      6      0.040189
      0      1      0.080378
      0      8      0.0013378
      2      2      3      3      68.00
      1      950.00013403
      1      98      0.000536      12
      0.70      0.46      0.50      1.00      1.0      1.0
1.0      1.0
      0      6      0.040189
      0      1      0.080378
      0      8      0.0013378
      3      2      3      3      68.00
      1      950.00013403
      1      98      0.000536      12
      0.70      0.46      0.50      1.00      1.0      1.0
1.0      1.0
      0      6      0.040189
      0      1      0.080378
      0      8      0.0013378
      4      2      3      3      68.00
      1      950.00013403
      1      98      0.000536      12
      0.70      0.46      0.50      1.00      1.0      1.0
1.0      1.0
      0      6      0.040189
      0      1      0.080378
      0      8      0.0013378
      5      2      3      3      68.00
      1      950.00013403
      1      98      0.000536      12
      0.70      0.46      0.50      1.00      1.0      1.0
1.0      1.0
      0      6      0.040189
      0      1      0.080378
      0      8      0.0013378
      6      0      1      3      68.00
      0      6      0.0878
      4      0      6      4      4      2      4      1      1      20      1      1      0
100
      0.0      0.0      0.0000      .0000001      0.0001      0
      1      5      0.5      0.0000      2      20      3.50      0.00000
      3      20      3.49      0.0000      4      20      3.50      0.00000
      5      20      3.49      0.0000      6      100      20.0      0.00000

```

“5 region sphere t400” DISNEL Code

```

0
19 1    AGN 201 equivalent sphere, 14.48 cm radius/fuse
      6      1      1
      1      2      3      3 71.941640
      1      950.00026804
      1      980.00107192 12
      0.89      0.46      0.50      1.00      1.0      1.0
1.0      1.0
      0      60.04018615
      0      10.08037230
      0      80.00133771
      2      2      3      3 71.742740
      1      950.00013402
      1      980.00053596 12
      0.70      0.46      0.50      1.00      1.0      1.0
1.0      1.0
      0      60.04018629
      0      10.08037258
      0      80.00133771
      3      2      3      3 71.145500
      1      950.00013402
      1      980.00053597 12
      0.70      0.46      0.50      1.00      1.0      1.0
1.0      1.0
      0      60.04018672
      0      10.08037345
      0      80.00133772
      4      2      3      3 70.092860
      1      950.00013402
      1      980.00053598 12
      0.70      0.46      0.50      1.00      1.0      1.0
1.0      1.0
      0      60.04018749
      0      10.08037497
      0      80.00133775
      5      2      3      3 68.703620
      1      950.00013403
      1      980.00053599 12
      0.70      0.46      0.50      1.00      1.0      1.0
1.0      1.0
      0      60.04018849
      0      10.08037698
      0      80.00133778
      6      0      1      3      68.00
      0      6      0.0878
      4      0      6      4      4      2      4      1      1      20      1      1      0
100
      0.0      0.0      0.0000      .0000001      0.0001      0
      1      50.50001182      0.0000      2      203.50007860      0.00000
      3      203.49006587      0.0000      4      203.50004395      0.00000
      5      203.49001473      0.0000      6      100      20.0      0.00000

```

“5 region sphere 100W” DISNEL Code

```

0
19 1    AGN 201 equivalent sphere, 14.48 cm radius/fuse
      6    1    1
      1    2    3    3152.936600
      1    950.00026765
      1    980.00107036    12
      0.89    0.46    0.50    1.00    1.0    1.0
1.0    1.0
      0    60.04012756
      0    10.08025511
      0    80.00133575
      2    2    3    3147.064460
      1    950.00013384
      1    980.00053524    12
      0.70    0.46    0.50    1.00    1.0    1.0
1.0    1.0
      0    60.04013180
      0    10.08026361
      0    80.00133590
      3    2    3    3134.316320
      1    950.00013387
      1    980.00053536    12
      0.70    0.46    0.50    1.00    1.0    1.0
1.0    1.0
      0    60.04014103
      0    10.08028205
      0    80.00133620
      4    2    3    3112.014860
      1    950.00013392
      1    980.00053558    12
      0.70    0.46    0.50    1.00    1.0    1.0
1.0    1.0
      0    60.04015716
      0    10.08031432
      0    80.00133674
      5    2    3    3    82.756220
      1    950.00013399
      1    980.00053586    12
      0.70    0.46    0.50    1.00    1.0    1.0
1.0    1.0
      0    60.04017833
      0    10.08035665
      0    80.00133744
      6    0    1    3    68.00
      0    6    0.0878
      4    0    6    4    4    2    4    1    1    20    1    1    0
100
      0.0    0.0    0.0000    .0000001    0.0001    0
      1    50.50025481    0.0000    2    203.50166035    0.00000
      3    203.49138866    0.0000    4    203.50092431    0.00000
      5    203.49030900    0.0000    6    100    20.0    0.00000

```